

---

# Alternating Local Enumeration (TnALE): Solving Tensor Network Structure Search with Fewer Evaluations

---

Chao Li<sup>1</sup> Junhua Zeng<sup>\*21</sup> Chunmei Li<sup>\*34</sup> Cesar Caiafa<sup>51</sup> Qibin Zhao<sup>1</sup>

## Abstract

Tensor network (TN) is a powerful framework in machine learning, but selecting a good TN model, known as TN structure search (TN-SS), is a challenging and computationally intensive task. The recent approach TNLS (Li et al., 2022) showed promising results for this task, however, its computational efficiency is still unaffordable, requiring too many evaluations of the objective function. We propose TnALE, a new algorithm that updates each structure-related variable alternately by local enumeration, *greatly* reducing the number of evaluations compared to TNLS. We theoretically investigate the descent steps for TNLS and TnALE, proving that both algorithms can achieve linear convergence up to a constant if a sufficient reduction of the objective is *reached* in each neighborhood. We also compare the evaluation efficiency of TNLS and TnALE, revealing that  $\Omega(2^N)$  evaluations are typically required in TNLS for *reaching* the objective reduction in the neighborhood, while ideally  $O(N^2R)$  evaluations are sufficient in TnALE, where  $N$  denotes the tensor order and  $R$  reflects the “low-rankness” of the neighborhood. Experimental results verify that TnALE can find practically good TN-ranks and permutations with vastly fewer evaluations than the state-of-the-art algorithms.

## 1. Introduction

Tensor network (TN) has been widely applied to solving high-dimensional problems in both machine learning (Anandkumar et al., 2014; Novikov et al., 2015; Zhe et al., 2015; Glasser et al., 2019; Kossaifi et al., 2020; Miller et al., 2021; Richter et al., 2021; Malik, 2022) and quantum physics (Orús, 2019). The success of *AlphaTensor* (Fawzi et al., 2022) once again confirmed the usefulness of tensors in both scientific and engineering fields. TN practitioners, on the other hand, have to face with challenging problems associated with model selection, known as *TN structure search (TN-SS)*, for example: (1) how to determine the TN-ranks?; (2) should we prefer tensor-train (TT, Oseledets 2011), tensor-ring (TR, Zhao et al. 2016) or other TN topology?; (3) how to relate the tensor modes to each core of a TN (permutation problem, Li et al. 2022), and so on. Unfortunately, some of these problems have been proven to be NP-hard (Hillar & Lim, 2013)<sup>1</sup>, and most of them suffer from the “combinatorial explosion”<sup>2</sup> so that the full exhaustive search is impossible in practice.

Several works have put effort into different aspects of the TN-SS (see Section 1.1), but many of the methods are restricted to specific tasks or work poorly in practice, so a general and efficient TN-SS method is needed. Recently, Li et al. (2022) proposed an algorithm dubbed TNLS, which can deal with the rank and permutation selection problem for TNs. However, its computational complexity is high since it requires evaluating the objective function on large batches of structure candidates.

To address this issue, we accelerate TNLS by equipping the algorithm with *Alternating Local Enumeration* — a simple but efficient searching method in neighborhoods. The new algorithm, named *TnALE*, can improve the evaluation efficiency of TNLS *greatly*. To be specific, TnALE follows the “local-searching” scheme as TNLS but alternately updates each variable of the TN structure by enumerating all values within a neighborhood. The intuition is that the alternately

---

<sup>\*</sup>Equal contribution <sup>1</sup>RIKEN Center for Advanced Intelligence Project (AIP), Tokyo, Japan <sup>2</sup>School of Automation, Guangdong University of Technology, Guangzhou, China <sup>3</sup>College of Information and Communication Engineering, Harbin Engineering University, Harbin, China <sup>4</sup>Department of Computer Science and Communications Engineering, WASEDA University, Tokyo, Japan <sup>5</sup>Instituto Argentino de Radioastronomía, CONICET CCT La Plata/CIC-PBA/UNLP, V. Elisa, ARGENTINA. . Correspondence to: Chao Li <chao.li@riken.jp>, Qibin Zhao <qibin.zhao@riken.jp>.

<sup>1</sup>For example, it proves that determining the optimal ranks for Tucker decomposition is NP-hard.

<sup>2</sup>It means the rapid growth of TN structure searching space due to the combinatorics of ranks, topologies or permutations, etc.

updating avoids the combinatorial explosion and the enumeration in neighborhoods guarantees the non-increasing of values of the objective in the search. On the other hand, the original TNLS applies random sampling, causing that many evaluations cannot provide useful information for decreasing the objective function.

The theoretical advantage of TnALE is also clear. We prove that, with new-defined *discrete* convexity-related assumptions of the objective function, both TNLS and TnALE can achieve a linear convergence up to a constant if a sufficient reduction of the objective function is reached in each neighborhood (Theorem 4.5). We also prove that TNLS requires the number of evaluations in the neighborhood to grow *exponentially* with the TN size (Prop. 4.8), determined by the dimension of the TN-ranks and the TN order, while TnALE grows with the TN size just *polynomially* in the ideal case (Prop. 4.8). Our analysis also reveals that such an improvement of the evaluation efficiency essentially comes from the *low-rankness* of the optimization landscape in neighborhoods, attributed to the close relationship between TnALE and cross-approximation methods for matrices and tensors (Tyrtshnikov, 2000; Oseledets & Tyrtshnikov, 2010; Sozykin et al., 2022). Numerically, extensive experiments on both synthetic and real-world data are implemented to verify the evaluation efficiency and the superior performance provided by TnALE.

Our main contributions can be summarized as follows:

- We propose a new algorithm named *TnALE*, which *greatly* reduces the evaluation cost of TNLS for the task of TN structure search;
- We establish for the first time the convergence analysis for both TNLS and TnALE, and rigorously prove their evaluation efficiency.

### 1.1. Related Works

**Tensor network structure search (TN-SS).** TN-SS can be classified into three sub-problems: (1) TN-rank selection (TN-RS) (Rai et al., 2014; Zhao et al., 2015; Yokota et al., 2016; Cheng et al., 2020; Mickelin & Karaman, 2020; Cai & Li, 2021; Hawkins & Zhang, 2021; Long et al., 2021; Sedighin et al., 2021; Yin et al., 2022); (2) TN-topology selection (TN-TS) (Falcó et al., 2020; Hashemizadeh et al., 2020; Kodryan et al., 2020; Li & Sun, 2020; Haberstick et al., 2021; Nie et al., 2021); and (3) TN-permutation selection (TN-PS) (Chen et al., 2022; Li et al., 2022). Recently, some methods to solve the TN-SS problem were inspired by discrete optimization, *e.g.*, (Hayashi et al., 2019; Hashemizadeh et al., 2020; Li & Sun, 2020; Li et al., 2021; 2022; Solgi et al., 2022). Although these methods typically achieve higher precision than their counterparts in practice, they suffer from the expensive computational cost and the

lack of theoretical analysis. Our work follows the TNLS algorithm (Li et al., 2022) in this direction but develops a new approach to improving the computational efficiency of TNLS and filling in the missing theoretical analysis for convergence and evaluation efficiency.

**Finding the extreme entry value within a tensor.** As discussed later in Section 4.2, the *alternating local enumeration* method is technically equivalent to finding the minimum entry within a multidimensional landscape. Our work is strongly related to the recently published method TTOpt (Sozykin et al., 2022), which finds the near-maximum entry of a tensor by cross-sampling (Tyrtshnikov, 2000; Zhang, 2019) in TT topology (Oseledets & Tyrtshnikov, 2010) and has been applied to various tasks (Nikitin et al., 2022; Shetty et al., 2022). Compared to TTOpt, the proposed TnALE recursively finds the minimum entry within a tensor associated with the neighborhood rather than the global search space, so that TnALE can handle the situation of *infinite* candidates (entries) in the optimization.

## 2. Preliminaries

In this section, we first summarize notations and review several central concepts related to the tensor network structure search (TN-SS). Then, we provide a quick review of TNLS (Li et al., 2022), a recently proposed algorithm for solving TN-SS, and point out that *TNLS suffers from the curse of dimensionality* in evaluation efficiency.

### 2.1. Notations

Throughout the paper, we typically use blackboard letters to denote sets of subjects, *e.g.*,  $\mathbb{G}, \mathbb{F}$ . In particular,  $\mathbb{R}, \mathbb{Z}_+$  and  $\mathbb{Z}_{\geq 0}$  denote real numbers, positive integers and non-negative integers, respectively. We use boldface letters to denote vectors and matrices, *e.g.*,  $\mathbf{x} \in \mathbb{Z}_+^K$  and  $\mathbf{A} \in \mathbb{R}^{I \times J}$ . For tensors of *arbitrary* order, we denote them using calligraphic letters, *e.g.*,  $\mathcal{A}, \mathcal{B} \in \mathbb{R}^{I_1 \times I_2 \times \dots \times I_N}$ . Given a vector, such as  $\mathbf{x} \in \mathbb{Z}_+^K$ ,  $\|\mathbf{x}\|$  and  $\|\mathbf{x}\|_\infty$  denote the  $l_2$ -norm and  $l_\infty$ -norm of  $\mathbf{x}$ , respectively. The norms are also directly applied to matrices and tensors by thinking of them as vectors. Following the notational convenience,  $|x|$  denotes the absolute value of  $x$  if  $x \in \mathbb{R}$  is a scalar, while  $|\mathbb{A}|$  denotes the cardinality if  $\mathbb{A}$  is a set. For the normed vector spaces armed with  $\|\mathbf{x}\|_\infty$ , we use  $B_\infty(\mathbf{x}, r_x)$  to denote the neighborhoods centered at  $\mathbf{x}$  with the radius  $r_x > 0$ . For any two functions  $f: \mathbb{B} \rightarrow \mathbb{C}$  and  $g: \mathbb{A} \rightarrow \mathbb{B}$ , the operation  $f \circ g: \mathbb{A} \rightarrow \mathbb{C}$  denotes the function composition.

### 2.2. Tensor network structure search (TN-SS)

We consider the *tensor network* (TN, Ye & Lim, 2019) as a set of real tensors of the dimension  $I_1 \times I_2 \times \dots \times I_N$ ,

denoted  $TNS(G, \mathbf{r})$ , whose elements are in the form of contractions of *core tensors* (Cichocki et al., 2017), associated to the TN structure modeled by the pair  $(G, \mathbf{r})$ , where  $G = (V, E)$  denotes a simple graph of  $N$  vertices modeling the *TN-topology* (Li & Sun, 2020) and  $\mathbf{r} \in \mathbb{Z}_+^{|E|}$  is a vector, whose entries are edge labels of  $G$  corresponding to the *TN-ranks* (Ye & Lim, 2019).

*Tensor network structure search* (TN-SS) aims generally to find more compressed TN models for computational purposes while preserving the models’ expressivity. Furthermore, the more compressed TN models also imply the potential advantage for the generalization capability in learning tasks (Khavari & Rabusseau, 2021). Suppose a dataset  $D$  and the task-specific loss function  $\pi_D : \mathbb{R}^{I_1 \times I_2 \times \dots \times I_N} \rightarrow \mathbb{R}_+$  involving  $D$ . TN-SS is to solve the following bi-level discrete optimization problem

$$\min_{(G, \mathbf{r}) \in \mathbb{G} \times \mathbb{F}_G} \left( \phi(G, \mathbf{r}) + \lambda \cdot \min_{\mathcal{Z} \in TNS(G, \mathbf{r})} \pi_D(\mathcal{Z}) \right), \quad (1)$$

where  $G \in \mathbb{G}$  is a graph of  $N$  vertices and  $K$  edges,  $\mathbf{r} \in \mathbb{F}_G \subseteq \mathbb{Z}_+^K$ ,  $\phi : \mathbb{G} \times \mathbb{Z}_+^K \rightarrow \mathbb{R}_+$  represents the function measuring the model complexity of a TN whose structure is modeled by  $(G, \mathbf{r})$ , and  $\lambda > 0$  is a tuning parameter. The intuition of (1) is that, the inner minimization is to evaluate the task-specific expressivity for a TN structure, while the outer minimization is to find the optimal structure for the task by balancing the complexity and the expressivity of a TN model.

We remark that the formulation (1) can be specified as different TN-SS sub-problems by restricting the feasible set  $\mathbb{G} \times \mathbb{F}_G$  into different forms: for TN-PS, we let  $\mathbb{F}_G = \mathbb{Z}_+^K$  and  $\mathbb{G}$  be the set containing the isomorphic graphs to a “template” graph (Li et al., 2022); for TN-RS, it typically restricts  $G$  to be fixed, and only finds TN-ranks *i.e.*,  $\mathbb{F}_G = \mathbb{Z}_+^K$ ; last for TN-TS, however, it relaxes  $\mathbb{G}$  to be the set containing all possible simple graphs of  $N$  vertices and the set  $\mathbb{F}_G$  can be fixed (Li & Sun, 2020) or searchable as well (Hashemizadeh et al., 2020). Note from Ye & Lim (2019); Li & Zhao (2021) that TN-TS (with rank selection) essentially coincides with TN-RS of a “fully-connected” TN (Zheng et al., 2021).

### 2.3. TNLS: a discrete optimization approach to TN-PS

Recently, Li et al. (2022) proposed an algorithm called TNLS for solving (1) effectively by stochastic search (Spall, 2005). The core process of TNLS is reviewed in Alg. 1, from which we see that the candidate of the optimal TN structure is updated if the algorithm finds better structures within a neighborhood using *random sampling*. Although Li et al. (2022) illustrates the superiority of TNLS compared to its counterparts, the algorithm is still time-consuming as acknowledged in their work. To understand the reason, we theoretically observe that TNLS suffers from the curse of

---

**Algorithm 1** *The core process of TNLS* (Li et al., 2022).

---

**Initialize:** Randomly choose a TN structure as the center of the neighborhood.

**while** not convergence **do**

1. Sampling  $(G, \mathbf{r})$ ’s *randomly* in the neighborhood;
2. Evaluating the samples with the objective of (1);
3. Updating the center if better samples are reached.

**end while**

**Output:** The center of the neighborhood.

---

dimensionality, due to the random sampling. More specifically, we state that

*under reasonable conditions,  $\Omega(2^K/\epsilon)$  samples are required by random sampling (wrt. step 1 in Alg. 1) for achieving a constant probability  $Pr \geq \epsilon$  for decreasing the objective of (1) in a neighborhood, where  $\epsilon > 0$  and  $K$  denotes the dimension of the search space.*

A formal statement is deferred to Prop. 4.8. For the commonly-used TNs of order  $N$ , the number of samples can be rewritten as  $\Omega(2^N/\epsilon)$ , by the fact  $K = O(N)$  in these TNs (Li et al., 2022). It is known from Alg. 1 that the sampled structures should be evaluated by solving the inner minimization of (1), so the huge number of samples implies the prohibitive cost in the computation. To address this problem, we introduce a more sampling-efficient approach by replacing the random sampling in Alg. 1, to accelerate the search procedure for TN-SS with fewer evaluations.

### 3. TnALE: Accelerating TNLS via Alternating Local Enumeration

We present now the new searching algorithm dubbed *TnALE* for solving the TN-SS problem. In particular, we focus on the technical details of *alternating local enumeration* (ALE), which replaces the random sampling used in Alg. 1 as the key factor for algorithm acceleration. More details of TnALE, including the pseudocode and *etc.*, can be found in Appendix A.

In TnALE, we find better structure candidates within a neighborhood by updating each structure-related variable alternately. Figure 1 illustrates a TN-PS example of how ALE finds ranks and permutations within a neighborhood for tensor ring (TR) decomposition of order-4, where the permutations reflect the different connections of the four vertices in TR (see panel (a)). In the beginning, all structure-related variables, including  $r_{\{1,2,3,4\}}$  and  $G$ , are initialized with the center of the neighborhood. To start the search, TN structures are sampled by enumerating all values of  $r_1$  *within* the neighborhood while other variables are fixed. Next, these sampled TN structures are evaluated by calculating the objective of (1), and then  $r_1$  is updated right off by choosing

the one with the minimum objective in the samples. Following  $r_1$ , the same operation is applied to variables from  $r_2$  to  $G$  sequentially (see panel (b)). After updating  $G$ , we turn the updating direction backward from  $r_4$  to  $r_1$ , *i.e.*, in a “round-trip” manner (see panel (c)). Overall, the ALE will be stopped if all variables are not changed anymore. We empirically found that in practice, a *one-time* “round-trip” is sufficient to reach a good TN structure for the next iteration of neighborhoods (as the 3rd step of Alg. 1). Note that the operation of ALE for TN-RS and TN-TS is in the same fashion, except that the graph  $G$  will be fixed in TN-RS or enumerated in differently-defined neighborhoods in TN-TS by considering different TN-topologies. In TnALE, we follow Li et al. (2022) to construct the neighborhood of TN structures.

**Remark 3.1 (tricks).** An additional merit of using enumeration is the “*knowledge transfer*” capability (Hashemizadeh et al., 2020). We know increasing the TN-ranks would decrease *monotonically* the training loss in many learning tasks. Instead of evaluating each structure explicitly, it thus inspires us to accelerate the structure evaluation by reusing the knowledge of the well-trained core tensors and their corresponding loss. In particular, the acceleration in TnALE by the knowledge transfer trick is two-fold: one is to use the well-trained core tensors associated with the lower-rank structures to be the initialization for the higher-rank structures, as in Hashemizadeh et al. (2020); the other is to employ the *loss estimation* by linear interpolation in place of the explicit enumeration when updating the TN-ranks (see Appendix A.1). Although the loss estimation would be of no precision, it is helpful in the first 1-2 iterations of TnALE (with a large radius) as initialization for quickly finding a suitable structure candidate.

**Remark 3.2 (computational complexity).** TnALE is a *meta*-algorithm for TN-SS, in which the inner minimization of (1) can be solved by any practitioner-appointed algorithms. Therefore, the computational complexity of TnALE is determined by the number of evaluations of the objective required in the search procedure. Suppose the *TN size* to be order- $N$  with the TN-ranks of dimension  $K$ . Furthermore, suppose each rank-related variable  $r_i$  as in Figure 1 is enumerated in  $I$  values, *e.g.*, the interval  $[r_i - I/2, r_i + I/2]$ , and  $D$  times of the “round-trip” updates. Therefore, for the TN-RS problem, TnALE requires  $O(DKI)$  evaluations in one neighborhood; for TN-PS, it requires  $O(DKI + DN^2/2)$  evaluations since the neighborhood of  $G$  in TN-PS contains  $(N - 1)N/2$  elements (Li et al., 2022) in general; last for TN-TS,  $O(DN^2I)$  evaluations are required. In practice, the value of  $I$  is typically set to 3 or 5 and  $D = 1$  (as in the experiments).

In summary, the evaluation complexity of TnALE grows polynomially with the *TN size*, *i.e.*, the dimension of the TN-ranks  $K$  and the TN-order  $N$ . In the next section, we prove

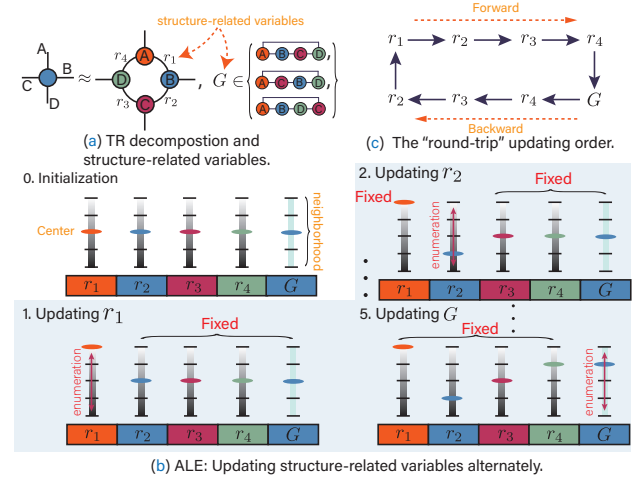


Figure 1. Illustration of *alternating local enumeration (ALE)* for TN-PS of TR decomposition. The search for TN-RS and TN-TS is similar, except that the ranges of the TN-ranks  $r_{\{1,2,3,4\}}$  and the graph  $G$  need to be adjusted.

that the number of evaluations in TnALE is theoretically sufficient for achieving a closely linear convergence rate for TN-SS.

## 4. Theoretical Results

In this section, we first analyze the descent steps for both TNLS and TnALE, proving that using the “local search” (Li et al., 2022) scheme the algorithms can achieve a linear convergence rate up to a constant if the objective is sufficiently “convex” in the *discrete* domain. Following this, we analyze the evaluation efficiency for TNLS and TnALE, showing that the required number of evaluations in TNLS would grow exponentially with the TN size, *i.e.*, the TN-order and the dimension of TN-ranks, while it can be ideally reduced to be a polynomial growth in TnALE if the neighborhood is *low-rank*. The proofs in this section are given in Appendix B.

### 4.1. Analysis of descent steps

We start the analysis by rewriting (1) into a more general form

$$\min_{\mathbf{x} \in \mathbb{Z}_+^K, p \in \mathbb{P}} f_p(\mathbf{x}) := f \circ p(\mathbf{x}), \quad (2)$$

where  $f : \mathbb{Z}_{>0}^L \rightarrow \mathbb{R}_+$  is a general form of the objective function of (1),  $\mathbf{x} \in \mathbb{Z}_+^K$  corresponds to the TN-ranks  $\mathbf{r}$  of (1), and the operator  $p : \mathbb{Z}_+^K \rightarrow \mathbb{Z}_{>0}^L$  and its feasible set  $\mathbb{P}$  correspond to the graph variable  $G$  and its feasible set  $\mathbb{G}$  of (1), respectively. The specific relationship of  $p$  and  $G$  is given in Appendix B.2.

The framework used in the proof follows from Golovin et al.

(2019) for the zeroth-order convex optimization. However, due to the discrete essence of (2), we re-establish discrete analogues of the fundamental concepts such as the gradient, strong convexity and smoothness for the analysis, and all the proofs are re-derived non-trivially in the discrete domain.

In doing so, we begin with the definition of the finite gradient (Olver, 2014), as the alternative to the classic gradient in the continuous domain.

**Definition 4.1 (finite gradient).** For any function  $f : \mathbb{Z}_{\geq 0}^L \rightarrow \mathbb{R}$ , its finite gradient  $\Delta f : \mathbb{Z}_{\geq 0}^L \rightarrow \mathbb{R}^L$  with respect to  $\mathbf{x} \in \mathbb{Z}_{\geq 0}^L$  is defined as follows:

$$\Delta f(\mathbf{x}) = [f(\mathbf{x} + \mathbf{e}_1) - f(\mathbf{x}), \dots, f(\mathbf{x} + \mathbf{e}_L) - f(\mathbf{x})]^\top, \quad (3)$$

where  $\mathbf{e}_i$ ,  $1 \leq i \leq L$  denote the unit vectors with the  $i$ -th entry being one and the others being zeros.

Next, we redefine the convexity and smoothness of the objective with finite gradients.

**Definition 4.2 ( $\alpha$ -strong convexity with finite gradient).** We say  $f$  is  $\alpha$ -strongly convex for  $\alpha \geq 0$  if  $f(\mathbf{y}) \geq f(\mathbf{x}) + \langle \Delta f(\mathbf{x}) - \frac{\alpha}{2} \mathbf{1}, \mathbf{y} - \mathbf{x} \rangle + \frac{\alpha}{2} \|\mathbf{y} - \mathbf{x}\|^2$  for all  $\mathbf{x}, \mathbf{y} \in \mathbb{Z}_{\geq 0}^L$ , where  $\mathbf{1} \in \mathbb{R}^L$  denotes the vector with all entries being one. We simply say  $f$  is convex if it is  $\alpha$ -strongly convex and  $\alpha = 0$ .

**Definition 4.3 ( $(\beta_1, \beta_2)$ -smoothness with finite gradient).** We say  $f$  is  $(\beta_1, \beta_2)$ -smooth for  $\beta_1, \beta_2 > 0$  if

1.  $|f(\mathbf{x}) - f(\mathbf{y})| \leq \beta_1 \|\mathbf{x} - \mathbf{y}\|$  for all  $\mathbf{x}, \mathbf{y} \in \mathbb{Z}_{\geq 0}^L$ ;
2. The function  $l(\mathbf{x}) := \frac{\beta_2}{2} \|\mathbf{x}\|^2 - f(\mathbf{x})$  is convex.

We remark that Definition 4.2 and 4.3 are partially different from the ones used in Golovin et al. (2019) or other literature for convex analysis. Particularly in Definition 4.3, the smoothness is defined by additionally taking the Lipschitz continuity (corresponding to *Item 1*) into account, which controls the changing rate of  $f$ , while *Item 2* in Definition 4.3 controls the changing rate of the finite gradient of  $f$ . See Lemma B.5 in Appendix for the proof. With the new definitions, we next give the main assumptions used in the results.

**Assumption 4.4.** Assume that  $f : \mathbb{Z}_{\geq 0}^L \rightarrow \mathbb{R}_+$  of (2) is  $\alpha$ -strongly convex,  $(\beta_1, \beta_2)$ -smooth, and its minimum, denoted  $(p^*, \mathbf{x}^*) = \arg \min_{p, \mathbf{x}} f \circ p(\mathbf{x})$ , satisfies  $\|\Delta f_{p^*}(\mathbf{x}^*) - \frac{\beta_2}{2} \mathbf{1}\| \leq \gamma$  where  $0 \leq \gamma < \alpha \leq \beta_1 \leq \beta_2 \leq 1$ .

In Assumption 4.4, the inequality  $\|\Delta f_{p^*}(\mathbf{x}^*) - \frac{\beta_2}{2} \mathbf{1}\| \leq \gamma$  implies that, up to a (small) bias  $\frac{\beta_2}{2} \mathbf{1}$ , the finite gradient at  $(p^*, \mathbf{x}^*)$  should be sufficiently small, which can be analogous to the ‘‘gradient-equal-zero’’ (Boyd & Vandenberghe,

2004) property of the stationary points for convex functions in the continuous domain. The upper bound ‘‘1’’ is arbitrarily chosen just for simplifying the calculation.

Next, we prove that the local-search scheme, used in both TNLS and TnALE, can achieve the linear convergence rate up to a constant. We first focus on TN-RS and TN-TS to simplify the problem, where  $p^*$  is assumed to be *known* beforehand. After that, we discuss TN-PS, showing that the searchable  $p$  would make the convergence more difficult.

**Theorem 4.5 (convergence rate when  $p^*$  is known).** *Suppose Assumption 4.4 is satisfied, the operator  $p$  of (2) is fixed to be  $p^*$ , and  $0 \leq \theta \leq 1$ . Then, for any  $\mathbf{x}$  with  $\|\mathbf{x} - \mathbf{x}^*\|_\infty \leq c$ , we can find a neighborhood  $B_\infty(\mathbf{x}, r_{\mathbf{x}})$  where  $r_{\mathbf{x}} \geq \theta c + \frac{1}{2}$ , such that there exists an element  $\mathbf{y} \in B_\infty(\mathbf{x}, r_{\mathbf{x}})$  satisfying*

$$f_{p^*}(\mathbf{y}) - f_{p^*}(\mathbf{x}^*) \leq (1 - \theta)(f_{p^*}(\mathbf{x}) - f_{p^*}(\mathbf{x}^*)) + \frac{7}{8}K. \quad (4)$$

Proving Theorem 4.5 requires the following lemma, which can be understood as the *discrete* version of the convex-combination inequality of convex functions.

**Lemma 4.6 (convex combination in the discrete domain).** *Suppose  $\mathbf{q} = \theta \mathbf{x} + (1 - \theta)\mathbf{y}$ ,  $\forall \mathbf{x}, \mathbf{y} \in \mathbb{Z}_{\geq 0}^L$ ,  $\theta \in [0, 1]$ , and there is  $\hat{\mathbf{q}} \in \mathbb{Z}_{\geq 0}^L$  following  $\Lambda = \mathbf{q} - \hat{\mathbf{q}}$ . If  $f$  is  $\alpha$ -strongly convex, then*

$$\theta f(\mathbf{x}) + (1 - \theta)f(\mathbf{y}) \geq f(\hat{\mathbf{q}}) + \left\langle \Delta f(\hat{\mathbf{q}}) - \frac{\alpha}{2} \mathbf{1}, \Lambda \right\rangle + \frac{\alpha}{2} \|\Lambda\|^2. \quad (5)$$

Note that the inequality (5) would be the same as the crucial inequality  $\theta f(\mathbf{x}) + (1 - \theta)f(\mathbf{y}) \geq f(\mathbf{q})$  in convex optimization if  $\Lambda = 0$ . However, due to  $\mathbf{q} \notin \mathbb{Z}_{\geq 0}^L$  in general even though  $\mathbf{x}, \mathbf{y} \in \mathbb{Z}_{\geq 0}^L$ , the non-zero  $\Lambda$  is inevitable in the proof, yielding the essential difference from the convex analysis in the continuous domain. As a consequence, the inequality (4) shows that the convergence rate is formally close to being linear, but the constant  $(7/8)K$  appears on the right-hand side, *dampening* the search efficiency.

Suppose the search trajectory  $\{f_{p^*}(\mathbf{x}_n)\}_{n=0}^\infty$ , of which the starting point  $\mathbf{x}_0 \in \mathbb{Z}_+^K$  is randomly chosen and  $\mathbf{x}_n$  for  $n > 0$  are determined by the vector  $\mathbf{y}$  in Theorem 4.5. As an important corollary, it can be easily proved that  $\{f_{p^*}(\mathbf{x}_n)\}_{n=0}^\infty$  converges to  $f_{p^*}(\mathbf{x}^*)$  up to a constant if  $\Omega(1/K) \leq \theta \leq 1$ . A rigorous proof for the convergence guarantee can be found in Appendix B.12.

**Remark 4.7 (Finding  $p^*$  makes the convergence slower.).** As aforementioned, the non-zero  $\|\Lambda\|_\infty$  decreases the search efficiency due to the additional constant shown in (4). It is known from the proof of Theorem 4.5 that the constant is derived from the tight bound  $\|\Lambda\|_\infty \leq 1/2$ , following the rounding operation. However, once the  $p$  in (2)

is searchable as well,  $\|\Lambda\|_\infty$  would turn larger, dampening the convergence more seriously. To verify this, suppose  $\mathbf{q} = \theta p^*(\mathbf{x}^*) + (1 - \theta)p_{\mathbf{x}}(\mathbf{x})$  to be the convex combination between  $(p^*, \mathbf{x}^*)$  and any point  $(p_{\mathbf{x}}, \mathbf{x})$ . It is known from the proof that, for decreasing the objective,  $\hat{\mathbf{q}}$  should satisfy  $\hat{\mathbf{q}} \in B_\infty(\mathbf{q}, \|\Lambda\|_\infty) \cap \mathbb{B}(p_{\mathbf{x}}, \mathbf{x})$ , where  $\mathbb{B}(p_{\mathbf{x}}, \mathbf{x}) := \{\mathbf{z} = \bar{p}(\bar{\mathbf{x}}) : \bar{p} \in B(p_{\mathbf{x}}), \bar{\mathbf{x}} \in B_\infty(\mathbf{x}, r_{\mathbf{x}})\}$  for some  $r_{\mathbf{x}} > 0$  and  $B(p_{\mathbf{x}})$  denotes the neighborhood of  $p_{\mathbf{x}}$  chosen in the algorithm. We thus see that, for the existence of  $\hat{\mathbf{q}}$ , the intersection  $B_\infty(\mathbf{q}, \|\Lambda\|_\infty) \cap \mathbb{B}(p_{\mathbf{x}}, \mathbf{x})$  should be non-empty. Following this, it satisfies  $\|\Lambda\|_\infty \geq \min_{\hat{\mathbf{q}} \in \mathbb{B}(p_{\mathbf{x}}, \mathbf{x})} \|\mathbf{q} - \hat{\mathbf{x}}\|_\infty \geq \min_{\hat{\mathbf{q}} \in \mathbb{Z}_{\geq 0}^L} \|\mathbf{q} - \hat{\mathbf{q}}\|_\infty = 1/2$  in the worst case. In this case, the larger value of  $\|\Lambda\|_\infty$  means a larger damping term appearing on the right-hand side of (4).

## 4.2. Evaluation efficiency

Note that a premise for achieving the closely linear convergence rate by TNLS and TnALE is that the expected  $\mathbf{y} \in B_\infty(\mathbf{x}, r_{\mathbf{x}})$  in Theorem 4.5 is reachable, meaning that the algorithms *should* find the  $\mathbf{y}$  out in each neighborhood. In the rest of the section, we show that TNLS is required to cost  $\Omega(2^K)$  samples in each neighborhood for stably reaching the  $\mathbf{y}$ , while  $O(KIR)$  samples are ideally sufficient for TnALE. Here  $K$  denotes the dimension of the search space (TN-ranks),  $I \in \mathbb{Z}_+$  indicates an integer related to the radius of the neighborhood and  $R \in \mathbb{Z}_+$  reflects the *low-rankness of the optimization landscape* in neighborhoods. We first give the proposition for TNLS as follows.

**Proposition 4.8 (curse of dimensionality for TNLS).** *Let the assumptions in Theorem 4.5 be satisfied. Furthermore, assume that  $\mathbf{x}^*$  is sufficiently smaller (or larger) than  $\mathbf{x}$  entry-wisely, except for a constant number of entries. Then the probability of achieving a suitable  $\mathbf{y}$  as mentioned in Theorem 4.5 by uniformly randomly sampling in  $B_\infty(\mathbf{x}, r_{\mathbf{x}})$  with  $r_{\mathbf{x}} \geq \theta c + \frac{1}{2}$  equals  $O(2^{-K})$ .*

Note that the additional assumption in Prop. 4.8 is commonly satisfied in practice when the searched TN-ranks are initialized uniformly with large (or small) values. It is also easily known from Prop. 4.8 that  $\Omega(2^K/\epsilon)$  samples are required for achieving the probability  $Pr \geq \epsilon$  for reaching the  $\mathbf{y}$  in the neighborhood.

*Remark 4.9.* The intuition of Prop. 4.8 is as follows. Suppose  $\mathbf{x}^*$  is entry-wisely smaller than  $\mathbf{x}$  without loss of generality, then the objective would be decreased only if most of the entries of  $\mathbf{x}$  are updated to be smaller values, *i.e.*, getting closer to  $\mathbf{x}^*$ . However, by random sampling, the probability of decreasing most entries of  $\mathbf{x}$  would turn smaller exponentially with increasing the dimension  $K$ , yielding the curse of dimensionality for TNLS.

In contrast to TNLS, TnALE essentially resolves the curse

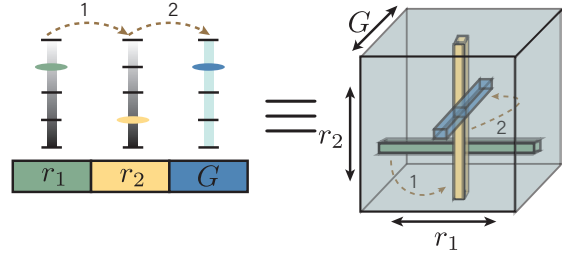


Figure 2. The relationship between alternating local enumeration (ALE) and TT-cross approximation (Oseledets & Tyrtshnikov, 2010; Sozykin et al., 2022). As shown in the figure, enumerating structure-related variables alternately is equivalent to sampling fibers of a tensor along each mode. The yellow arrows indicate the alternation of variables from  $r_1$  to  $r_2$  and then to  $G$ , respectively.

of dimensionality by leveraging the landscape’s low-rank structure. To verify this, given  $(p, \mathbf{x})$ , we formulate first the neighborhood  $B(p) \times B_\infty(\mathbf{x}, r_{\mathbf{x}})$  as a  $(K + 1)$ -th order tensor  $\mathcal{B} \in \mathbb{R}^{I_1 \times I_2 \times \dots \times I_{K+1}}$ . Here  $I_k = 2 \times \lceil r_{\mathbf{x}} \rceil + 1$  for  $1 \leq k \leq K$  and  $I_{K+1} = |B(p)|$ . The  $(i_1, i_2, \dots, i_{K+1})$ -th entry of  $\mathcal{B}$ , written  $\mathcal{B}(\mathbf{i})$  with  $\mathbf{i} = [i_1, i_2, \dots, i_{K+1}]^\top$ , satisfies

$$\mathcal{B}(\mathbf{i}) = 1/f_{p_{i_{K+1}}}(\mathbf{x} + \mathbf{i}(:K) - (\lceil r_{\mathbf{x}} \rceil + 1)), \quad (6)$$

where  $\mathbf{i}(:K)$  denotes the  $K$ -dimensional vector consisting of the first  $K$  entries of  $\mathbf{i}$ , and  $p_{i_{K+1}}$  denotes the  $i_{K+1}$ -th element of  $B(p)$  in any ordering fashion. We remark that the inverse  $1/f(\mathbf{x})$  is always valid due to the assumption  $f_p(\mathbf{x}) > 0$  in (2) for all  $\mathbf{x}$  and  $p$ . We also remark that the equation (6) maps uniquely each element of  $B(p) \times B_\infty(\mathbf{x}, r_{\mathbf{x}})$  onto the entries of  $\mathcal{B}$ .

By the tensor  $\mathcal{B}$ , we can find that the proposed *alternating local enumeration (ALE)* is strongly related to TT-cross (Oseledets & Tyrtshnikov, 2010) and TTOpt (Sozykin et al., 2022). As demonstrated in Figure 2, the enumeration for each variable is equivalent to drawing a fiber of  $\mathcal{B}$  as in TT-cross or TTOpt with the TT-ranks being *ones*. Such a relationship helps us reveal the evaluation advantage of TnALE. Specifically, let  $\mathbb{B} := B(p) \times B_\infty(\mathbf{x}, r_{\mathbf{x}})$  and  $f_{\mathbb{B}}^* := \min_{(p_{\mathbf{y}}, \mathbf{y}) \in \mathbb{B}} f_{p_{\mathbf{y}}}(\mathbf{y})$  for notational simplicity, then we have the following proposition.

**Proposition 4.10 (evaluation efficiency for TnALE).** *Let  $\mathcal{B} \in \mathbb{R}^{I_1 \times I_2 \times \dots \times I_{K+1}}$  be the tensor of order- $(K + 1)$  constructed as Eq. (6) with  $I_1 = I_2 = \dots = I_{K+1} = I$  for simplicity. Then, there exists its TT-cross approximation (Oseledets & Tyrtshnikov, 2010) of rank- $R^3$ , denoted  $\hat{\mathcal{B}}$ , such that  $f_{\hat{\mathcal{B}}}^* = f_{p_{j_{K+1}}}(\mathbf{x} + \mathbf{j}(:K) - (\lceil r_{\mathbf{x}} \rceil + 1))$  with*

<sup>3</sup>Here we assume that all elements of the TT-ranks are equal to  $R$  for brevity.

$\mathbf{j} = \arg \max_{\mathbf{i}} \hat{\mathcal{B}}(\mathbf{i})$  holds, provided that

$$f_{\mathbb{B}}^* \leq f_{p_z}(\mathbf{z}) / \left( 1 + 2 \frac{(4R)^{\lceil \log_2 K \rceil} - 1}{4R - 1} (R + 1)^2 \xi f_{p_z}(\mathbf{z}) \right) \quad (7)$$

for all  $(p_z, \mathbf{z}) \in \mathbb{B}$  and  $f_{p_z}(\mathbf{z}) \neq f_{\mathbb{B}}^*$ . Here,  $\xi$  denotes the error between  $\mathcal{B}$  and its best approximation of TT-ranks  $R$  in terms of  $\|\cdot\|_{\infty}$ . Note that the inequality (7) holds trivially if  $\mathcal{B}$  is exactly of the TT topology of rank- $R$ , and Oseledets & Tyrtyshnikov (2010) shows that the  $f_{\mathbb{B}}^*$  can be recovered from  $O(KIR)$  entries from  $\mathcal{B}$ .

Prop. 4.10 is a natural corollary of Theorem 2 in Osinsky (2019). It implies that the desired  $\mathbf{y}$  (corresponding to  $f_{\mathbb{B}}^*$  in Prop. 4.10) in Theorem 4.5 is reachable by only  $O(KIR)$  samples once  $\mathcal{B}$  is of TT with rank- $R$ . Even though  $\mathcal{B}$  is not low-rank, the  $\mathbf{y}$  can still be located if the inequality (7) is satisfied. For the three TN-SS sub-problems for TNs of order- $N$ , the number of the required samples can be specified as  $O(KIR)$  for TN-RS,  $O(KIR + N^2R/2)$  for TN-PS, and  $O(N^2IR)$  for TN-TS, respectively.

Prop. 4.10 shows the  $O(KIR)$  evaluation advantage compared with TNLS that requires  $\Omega(2^K/\epsilon)$  evaluations in the neighborhoods, but it remains open to prove the low-rankness of the optimization landscape in the TN-SS tasks. We empirically verify this with five synthetic tensors of order four. We calculate their complete optimization landscape associated with the  $l_2$  loss, observing that the multidimensional landscape is indeed low-rank under all possible unfoldings (see Figure 3 in Appendix). We thus conjecture that in practice the low-rank structure of the landscape should be preserved, at least in neighborhoods. In the next section, the evaluation advantage by TnALE will be empirically verified with both synthetic and real-world data.

## 5. Experimental Results

In this section, we present numerical results to verify the superiority of TnALE in terms of evaluation cost. Due to the page limit, the experimental settings will be presented at the minimum level for clarity. Additional details are given in Appendix C.

### 5.1. Synthetic data

First of all, we verify the superiority of TnALE by solving the TN-PS problem, in which both the optimal TN-ranks and permutations of synthetic tensors are searched for the tensor decomposition task.

In the experiment, we *re-use* from Li et al. (2022) the synthetic tensors, which are randomly generated in the topologies including TR (order-8), PEPS (order-6, Verstraete & Cirac, 2004), hierarchical Tucker (HT, Hackbusch & Kühn, 2009), and MERA (order-8, Cincio et al., 2008). Addi-

Table 1. Number of evaluations for the rank and permutation identification, where the symbol “-” in the table means the failure of the approach.

Topology	Methods	Data – #Eva. ↓			
		A	B	C	D
TR	TNGA	2850	2250	3900	1950
	TNLS	1020	960	1320	780
	Ours	<b>231</b>	<b>308</b>	<b>308</b>	<b>231</b>
PEPS	TNGA+	1560	-	840	1080
	TNLS	781	781	421	661
	Ours	<b>407</b>	<b>465</b>	<b>233</b>	<b>175</b>
HT	TNGA	960	1320	840	1080
	TNLS	841	841	781	721
	Ours	<b>211</b>	<b>281</b>	<b>211</b>	<b>211</b>
MERA	TNGA	-	960	2800	3240
	TNLS	1561	841	1441	721
	Ours	<b>1450</b>	<b>484</b>	<b>323</b>	<b>323</b>
TW	TNGA	1920	1440	600	720
	TNLS	661	601	601	481
	Ours	<b>285</b>	<b>143</b>	<b>285</b>	<b>214</b>

tionally, we also consider the *tensor wheel* model (TW of order-5, Wu et al., 2022). Since the mode dimension is typically irrelevant to the difficulty of TN-SS, we set them equalling 3 for all tensors. For each topology, there are four tensors (**A**, **B**, **C**, **D**), the TN-ranks and permutations are randomly selected and they remain unknown. The goal of this experiment is to compare different approaches to find the TN-ranks and permutations for each tensor, so that the conditions  $RSE \leq 10^{-4}$  and the  $Eff. \geq 1$  are satisfied<sup>4</sup>. Otherwise, we say the approach fails in the experiment.

We implemented three algorithms, TNGA (Li & Sun, 2020), TNLS and TnALE (ours). For a fair comparison, the three approaches use the same objective and solver for the inner minimization of (1). Furthermore, TNLS and TnALE are initialized with the same TN structures. The rest of the experimental settings remain as Li et al. (2022).

The experimental results are shown in Table 1. We see that both TNLS and TnALE (ours) successfully identify the ranks and permutations for all tensors. Furthermore, TnALE requires *significantly* fewer evaluations than both TNGA and TNLS. Figure 4 in Appendix further illustrates the objective (in log, averaged) versus the number of evaluations for TNLS and TnALE. It confirms the consistency of evaluation advantage of TnALE.

Next, we evaluate the performance of TnALE for solving the

<sup>4</sup>RSE means the relative squared error, and the *Eff.* index (Li & Sun, 2020) denotes the ratio of the parameter number of TNs between the searched structure and the one used in data generation.  $Eff. \geq 1$  implies that the algorithm finds a TN structure identical or more compact than the one used in data generation.

Table 2. Experimental results of TN-RS (rank-selection) in 8th-order TR topology. The columns of “lower-ranks” and “higher-ranks” indicate two regimes from which the TN-ranks are randomly selected, respectively. Each  $Eff.$  and [#Eva.] value is averaged using five tensors.

Methods	lower-ranks	higher-ranks
	$Eff.\uparrow$	$Eff.\uparrow$
TR-SVD	$0.65\pm 0.46$	$0.13\pm 0.20$
TR-BALS	$1.15\pm 0.14$	$0.19\pm 0.22$
TR-LM	$1.15\pm 0.14$	$0.15\pm 0.02$
TRAR	$0.55\pm 0.10$	$0.63\pm 0.06$
	$Eff.\uparrow$ [#Eva.↓]	$Eff.\uparrow$ [#Eva.↓]
TNGA	$1.08\pm 0.06$ [552]	$1.00\pm 0.00$ [900]
TNLS	$1.08\pm 0.06$ [492]	$1.00\pm 0.00$ [588]
TTOpt ( $R = 1$ )	$1.08\pm 0.06$ [104]	$1.00\pm 0.00$ [178]
TTOpt ( $R = 2$ )	$1.02\pm 0.02$ [314]	$1.00\pm 0.00$ [752]
Ours	$1.08\pm 0.06$ [80]	$1.00\pm 0.00$ [119]

classic rank selection problem, *i.e.*, TN-RS, for TR decomposition. To be specific, we randomly generate synthetic TR-tensors of order 8, and consider two configurations: “lower-ranks” and “higher-ranks”. In the “lower-ranks” class, the TN-ranks are randomly chosen in the interval  $[1, 4]$ , while in the “higher-ranks” class the selection interval is lifted to  $[5, 8]$ , so that the ranks would be larger than the tensors’ mode dimension (which equals 3 in this experiment). This situation commonly happens in practice for high-order TNs. For comparison, we implement various rank-adaptive TR decomposition methods, including TR-SVD and TR-BALS (Zhao et al., 2016), TR-LM (Mickelin & Karaman, 2020), and TRAR (Sedighin et al., 2021). In addition, the TTOpt algorithm (Sozykin et al., 2022) with ranks<sup>5</sup> equaling  $\{1, 2\}$  is also employed as a baseline.

The experimental results are shown in Table 2. We see that most of the methods can successfully identify the TN-ranks (implied by  $Eff.\geq 1$ ) in the “lower-ranks” class, but in the “higher-ranks” class only the methods at the bottom of the table manage to find the ranks. Furthermore, TnALE costs the fewest evaluations on average compared with TNGA, TNLS and TTOpt.

## 5.2. Real-world data

We apply now the proposed method to real-world data to compress the learnable parameters of the tensorial Gaussian process (TGP, Izmailov et al. 2018) and natural images. In TGP compression, we consider the regression task by TGPs for three datasets, including CCPP (Tüfekci, 2014), MG (Flake & Lawrence, 2002), and Protein (Dua & Graff, 2017), and compress the variational mean of the process with the TT/TR decomposition using the same setting as

<sup>5</sup>Here the ranks are tuning parameters in the TTOpt algorithm.

Table 3. Number of parameters ( $\times 1000$ , ↓) and MSE (in round brackets) for TGP model compression, where the values in [square brackets] show the number of evaluations required in each method.

	CCPP	MG	Protein
TGP	2.64 (0.06) [N/A]	3.36 (0.33) [N/A]	2.88 (0.74) [N/A]
TNGA	<b>2.24</b> (0.06) [1500]	<b>3.01</b> (0.33) [4900]	2.03 (0.74) [3900]
TNLS	<b>2.24</b> (0.06) [1051]	<b>3.01</b> (0.33) [3901]	<b>1.88</b> (0.74) [3601]
Ours	<b>2.24</b> (0.06) [124]	<b>3.01</b> (0.33) [276]	<b>1.88</b> (0.74) [1053]

Table 4. Results for natural image compression. The underlined values show the best compression ratio achieved in the same RSE.

Tasks	Methods	Data - compression ratio (log, ↑) (RSE ↓) [#Eva. ↓]			
		A	B	C	D
TN-PS	TNGA	1.10 (0.15) [8400]	1.37 (0.17) [6300]	1.77 (0.08) [4800]	1.47 (0.10) [5100]
	TNLS	1.09 (0.16) [1351]	<u>1.41</u> (0.17) [1501]	1.71 (0.08) [2551]	1.47 (0.10) [2101]
	Ours	1.14 (0.16) [647]	1.39 (0.17) [666]	<u>1.80</u> (0.08) [394]	<u>1.49</u> (0.10) [444]
TN-TS	Greedy	0.81 (0.16)	0.97 (0.17)	1.44 (0.08)	0.68 (0.10)
	TNGA	1.16 (0.16) [2100]	<u>1.48</u> (0.17) [1800]	<u>1.81</u> (0.08) [1900]	1.48 (0.09) [1000]
	TNLS	1.15 (0.16) [1300]	1.40 (0.17) [1100]	1.80 (0.08) [1700]	1.50 (0.10) [1700]
	Ours	1.10 (0.15) [177]	1.46 (0.17) [153]	<u>1.81</u> (0.08) [237]	1.51 (0.10) [246]

in Li et al. (2022). The goal of the experiment is to search good TN-ranks and permutations for using fewer parameters to achieve the same mean square error (MSE) in regression. The experimental results are shown in Table 3. We can see that TnALE achieves the same compression ratio as TNGA and TNLS but costs *significantly* fewer evaluations than the counterparts in factor up to 14 (3901/276).

Last, we consider the TN-PS and TN-TS tasks for compressing natural images. In TN-TS, we search for good TN-ranks and topologies for image compression. In the experiment, we randomly select four images (A, B, C, D) from the dataset BSD500 (Arbelaez et al., 2010). Each image is resized by  $256 \times 256$  and then reshaped into an order-8 tensor. For comparison, we also implement the “Greedy” method (Hashemizadeh et al., 2020) for TN-TS. Table 4 shows the results, including the compression ratio, RSE and the evaluation cost in both tasks. We see that TnALE achieves the closest compression ratio and RSE to TNGA and TNLS but it required much fewer evaluations.

## 6. Concluding Remarks

Extensive experimental results demonstrate that the proposed TnALE approach can *greatly* reduce the evaluation cost, up to  $10\times$  fewer evaluations, compared with TNLS (Li et al., 2022) and other methods for the task of tensor network structure search (TN-SS). The theoretical results in this pa-

per provide a rigorous analysis of the convergence rate and the evaluation efficiency for both TNLS and TnALE.

**Limitation.** The main limitation of TnALE is the local convergence issue. In particular, we empirically found in the TN-TS experiment (see Table (4)) multiple local minima, which are poor in compression ratio, and TnALE can easily drop in them. Instead, the methods TNGA (Li & Sun, 2020) and TNLS (Li et al., 2022) seem to better avoid local minima, owing to their stochastic essence. Solving this issue will be the direction of our future work.

## References

- Anandkumar, A., Ge, R., Hsu, D., Kakade, S. M., and Telgarsky, M. Tensor decompositions for learning latent variable models. *The Journal of Machine Learning Research*, 15(1):2773–2832, 2014.
- Arbelaez, P., Maire, M., Fowlkes, C., and Malik, J. Contour detection and hierarchical image segmentation. *IEEE transactions on pattern analysis and machine intelligence*, 33(5):898–916, 2010.
- Boyd, S. and Vandenberghe, L. *Convex optimization*. Cambridge university press, 2004.
- Cai, Y. and Li, P. A blind block term decomposition of high order tensors. In *Proceedings of the AAAI Conference on Artificial Intelligence*, number 8, pp. 6868–6876, 2021.
- Chen, Z., Lu, J., and Zhang, A. R. One-dimensional tensor network recovery. *arXiv preprint arXiv:2207.10665*, 2022.
- Cheng, Z., Li, B., Fan, Y., and Bao, Y. A novel rank selection scheme in tensor ring decomposition based on reinforcement learning for deep neural networks. In *ICASSP 2020-2020 IEEE International Conference on Acoustics, Speech and Signal Processing (ICASSP)*, pp. 3292–3296. IEEE, 2020.
- Cichocki, A., Phan, A.-H., Zhao, Q., Lee, N., Oseledets, I., Sugiyama, M., Mandic, D. P., et al. Tensor networks for dimensionality reduction and large-scale optimization: Part 2 applications and future perspectives. *Foundations and Trends® in Machine Learning*, 9(6):431–673, 2017.
- Cincio, L., Dziarmaga, J., and Rams, M. M. Multiscale entanglement renormalization ansatz in two dimensions: quantum Ising model. *Physical Review Letters*, 100(24):240603, 2008.
- Dua, D. and Graff, C. UCI machine learning repository, 2017. URL <http://archive.ics.uci.edu/ml>.
- Falcó, A., Nouy, W. H., et al. Geometry of tree-based tensor formats in tensor banach spaces. *arXiv preprint arXiv:2011.08466*, 2020.
- Fawzi, A., Balog, M., Huang, A., Hubert, T., Romera-Paredes, B., Barekatin, M., Novikov, A., Ruiz, F. J. R., Schrittwieser, J., Swirszcz, G., Silver, D., Hassabis, D., and Kohli, P. Discovering faster matrix multiplication algorithms with reinforcement learning. *Nature*, 610(7930):47–53, 2022.
- Flake, G. W. and Lawrence, S. Efficient SVM regression training with SMO. *Machine Learning*, 46(1):271–290, 2002.
- Glasser, I., Sweke, R., Pancotti, N., Eisert, J., and Cirac, I. Expressive power of tensor-network factorizations for probabilistic modeling. *Advances in neural information processing systems*, 32, 2019.
- Golovin, D., Karro, J., Kochanski, G., Lee, C., Song, X., and Zhang, Q. Gradientless descent: High-dimensional zeroth-order optimization. In *International Conference on Learning Representations*, 2019.
- Haberstich, C., Nouy, A., and Perrin, G. Active learning of tree tensor networks using optimal least-squares. *arXiv preprint arXiv:2104.13436*, 2021.
- Hackbusch, W. and Kühn, S. A new scheme for the tensor representation. *Journal of Fourier analysis and applications*, 15(5):706–722, 2009.
- Hashemizadeh, M., Liu, M., Miller, J., and Rabusseau, G. Adaptive tensor learning with tensor networks. *arXiv preprint arXiv:2008.05437*, 2020.
- Hawkins, C. and Zhang, Z. Bayesian tensorized neural networks with automatic rank selection. *Neurocomputing*, 453:172–180, 2021.
- Hayashi, K., Yamaguchi, T., Sugawara, Y., and Maeda, S.-i. Exploring unexplored tensor network decompositions for convolutional neural networks. In *Advances in Neural Information Processing Systems*, pp. 5553–5563, 2019.
- Hillar, C. J. and Lim, L.-H. Most tensor problems are NP-hard. *Journal of the ACM (JACM)*, 60(6):45, 2013.
- Izmailov, P., Novikov, A., and Kropotov, D. Scalable Gaussian processes with billions of inducing inputs via tensor train decomposition. In *International Conference on Artificial Intelligence and Statistics*, pp. 726–735. PMLR, 2018.
- Khavari, B. and Rabusseau, G. Lower and upper bounds on the pseudo-dimension of tensor network models. *Advances in Neural Information Processing Systems*, 34, 2021.
- Kingma, D. P. and Ba, J. Adam: A method for stochastic optimization. *arXiv preprint arXiv:1412.6980*, 2014.

- Kodryan, M., Kropotov, D., and Vetrov, D. MARS: Masked automatic ranks selection in tensor decompositions. *arXiv preprint arXiv:2006.10859*, 2020.
- Kossaifi, J., Lipton, Z. C., Kolbeinsson, A., Khanna, A., Furlanello, T., and Anandkumar, A. Tensor regression networks. *Journal of Machine Learning Research*, 21: 1–21, 2020.
- Li, C. and Sun, Z. Evolutionary topology search for tensor network decomposition. In *Proceedings of the 37th International Conference on Machine Learning (ICML)*, 2020.
- Li, C. and Zhao, Q. Is rank minimization of the essence to learn tensor network structure? In *Second Workshop on Quantum Tensor Networks in Machine Learning (QT-NML)*, Neurips, 2021.
- Li, C., Zeng, J., Tao, Z., and Zhao, Q. Permutation search of tensor network structures via local sampling. In *International Conference on Machine Learning*, pp. 13106–13124. PMLR, 2022.
- Li, N., Pan, Y., Chen, Y., Ding, Z., Zhao, D., and Xu, Z. Heuristic rank selection with progressively searching tensor ring network. *Complex & Intelligent Systems*, pp. 1–15, 2021.
- Long, Z., Zhu, C., Liu, J., and Liu, Y. Bayesian low rank tensor ring for image recovery. *IEEE Transactions on Image Processing*, 30:3568–3580, 2021.
- Malik, O. A. More efficient sampling for tensor decomposition with worst-case guarantees. In *International Conference on Machine Learning*, pp. 14887–14917. PMLR, 2022.
- Mickelin, O. and Karaman, S. On algorithms for and computing with the tensor ring decomposition. *Numerical Linear Algebra with Applications*, 27(3):e2289, 2020.
- Miller, J., Rabusseau, G., and Terilla, J. Tensor networks for probabilistic sequence modeling. In *International Conference on Artificial Intelligence and Statistics*, pp. 3079–3087. PMLR, 2021.
- Nie, C., Wang, H., and Tian, L. Adaptive tensor networks decomposition. In *BMVC*, 2021.
- Nikitin, A., Chertkov, A., Ballester-Ripoll, R., Oseledets, I., and Frolov, E. Are quantum computers practical yet? a case for feature selection in recommender systems using tensor networks. *arXiv preprint arXiv:2205.04490*, 2022.
- Novikov, A., Podoprikin, D., Osokin, A., and Vetrov, D. P. Tensorizing neural networks. In *Advances in Neural Information Processing Systems*, pp. 442–450, 2015.
- Olver, P. J. *Introduction to partial differential equations*. Springer, 2014.
- Orús, R. Tensor networks for complex quantum systems. *Nature Reviews Physics*, 1(9):538–550, 2019.
- Oseledets, I. and Tyrtyshenikov, E. TT-cross approximation for multidimensional arrays. *Linear Algebra and its Applications*, 432(1):70–88, 2010.
- Oseledets, I. V. Tensor-train decomposition. *SIAM Journal on Scientific Computing*, 33(5):2295–2317, 2011.
- Osinsky, A. Tensor trains approximation estimates in the chebyshev norm. *Computational Mathematics and Mathematical Physics*, 59(2):201–206, 2019.
- Rai, P., Wang, Y., Guo, S., Chen, G., Dunson, D., and Carin, L. Scalable bayesian low-rank decomposition of incomplete multiway tensors. In *International Conference on Machine Learning*, pp. 1800–1808. PMLR, 2014.
- Richter, L., Sallandt, L., and Nüsken, N. Solving high-dimensional parabolic PDEs using the tensor train format. In Meila, M. and Zhang, T. (eds.), *Proceedings of the 38th International Conference on Machine Learning*, pp. 8998–9009. PMLR, 2021.
- Sedighin, F., Cichocki, A., and Phan, A.-H. Adaptive rank selection for tensor ring decomposition. *IEEE Journal of Selected Topics in Signal Processing*, 15(3):454–463, 2021.
- Shetty, S., Lembono, T., Loew, T., and Calinon, S. Tensor train for global optimization problems in robotics. *arXiv preprint arXiv:2206.05077*, 2022.
- Snyder, L. V. and Daskin, M. S. A random-key genetic algorithm for the generalized traveling salesman problem. *European journal of operational research*, 174(1):38–53, 2006.
- Solgi, R., Loaiciga, H. A., and Zhang, Z. Evolutionary tensor train decomposition for hyper-spectral remote sensing images. In *IGARSS 2022-2022 IEEE International Geoscience and Remote Sensing Symposium*, pp. 1145–1148. IEEE, 2022.
- Sozykin, K., Chertkov, A., Schutski, R., Phan, A.-H., Cichocki, A., and Oseledets, I. TTOpt: A maximum volume quantized tensor train-based optimization and its application to reinforcement learning. *arXiv preprint arXiv:2205.00293*, 2022.
- Spall, J. C. *Introduction to stochastic search and optimization: estimation, simulation, and control*. John Wiley & Sons, 2005.

- Tüfekci, P. Prediction of full load electrical power output of a base load operated combined cycle power plant using machine learning methods. *International Journal of Electrical Power & Energy Systems*, 60:126–140, 2014.
- Tyrtshnikov, E. Incomplete cross approximation in the mosaic-skeleton method. *Computing*, 64(4):367–380, 2000.
- Verstraete, F. and Cirac, J. I. Renormalization algorithms for quantum-many body systems in two and higher dimensions. *arXiv preprint cond-mat/0407066*, 2004.
- Wang, W., Aggarwal, V., and Aeron, S. Efficient low rank tensor ring completion. In *Proceedings of the IEEE International Conference on Computer Vision*, pp. 5697–5705, 2017.
- Wu, Z.-C., Huang, T.-Z., Deng, L.-J., Dou, H.-X., and Meng, D. Tensor wheel decomposition and its tensor completion application. In *Advances in Neural Information Processing Systems*, 2022.
- Ye, K. and Lim, L.-H. Tensor network ranks. *arXiv preprint arXiv:1801.02662*, 2019.
- Yin, M., Phan, H., Zang, X., Liao, S., and Yuan, B. Batude: Budget-aware neural network compression based on Tucker decomposition. In *Proceedings of the AAAI Conference on Artificial Intelligence*, volume 1, 2022.
- Yokota, T., Zhao, Q., and Cichocki, A. Smooth PARAFAC decomposition for tensor completion. *IEEE Transactions on Signal Processing*, 64(20):5423–5436, 2016.
- Zhang, A. Cross: Efficient low-rank tensor completion. *The Annals of Statistics*, 47(2):936–964, 2019.
- Zhao, Q., Zhang, L., and Cichocki, A. Bayesian CP factorization of incomplete tensors with automatic rank determination. *IEEE transactions on pattern analysis and machine intelligence*, 37(9):1751–1763, 2015.
- Zhao, Q., Zhou, G., Xie, S., Zhang, L., and Cichocki, A. Tensor ring decomposition. *arXiv preprint arXiv:1606.05535*, 2016.
- Zhe, S., Xu, Z., Chu, X., Qi, Y., and Park, Y. Scalable nonparametric multiway data analysis. In *Artificial Intelligence and Statistics*, pp. 1125–1134. PMLR, 2015.
- Zheng, Y.-B., Huang, T.-Z., Zhao, X.-L., Zhao, Q., and Jiang, T.-X. Fully-connected tensor network decomposition and its application to higher-order tensor completion. In *Proc. AAAI*, volume 35, pp. 11071–11078, 2021.

## A. TnALE: Details for the algorithm

The pseudocode for ALE is given in Alg. 3. As discussed in the paper, each structure-related variable is updated alternately by enumeration in the neighborhood. Based on it, the entire algorithm of TnALE is shown in Alg. 2. Apart from the major iteration (lines 6-8), beforehand, there is an initial phase, where we apply a larger radius  $r_1$  and the objective prediction trick to find the candidates in a broader range and a rough fashion.

### A.1. The loss estimation trick.

As discussed in Remark 3.1, we employ the *loss estimation* by linear interpolation in place of the complete enumeration when updating the TN-ranks. Particularly in Alg. 2, we apply this trick to the initial phase, where we consider a broader range of the neighborhood for roughly finding the structure candidates.

Suppose a rank variable  $r$  is required to be enumerated in the range of  $r_0 - b \leq r \leq r_0 + b$ , where  $r_0, b \in \mathbb{Z}_+$  present the center and radius of the searched neighborhood, respectively. The loss estimation trick aims to estimate the minimum of the inner optimization of (1) associated with each enumerated TN-structures with limited evaluations. In the trick, we first evaluate explicitly three TN structures, *i.e.*,  $r = \{r_0 - b, r_0, r_0 + b\}$ . Then, a simple linear regression model would predict the evaluations of TN-structures in the interval  $(r_0, r_0 + b)$  using the data of  $\{r_0, r_0 + b\}$ . The evaluations for the interval  $(r_0 - b, r_0)$  will be predicted similarly using the data of  $\{r_0 - b, r_0\}$ . We can see from the trick that the inner minimization of (1) can be quickly estimated with only three explicit evaluations, no matter how wide the searching range is. Although the simple linear regression can only give a rough estimation, it is sufficiently helpful for TnALE to find good TN-structures in the initial phase.

### A.2. The neighborhood in the graph space

In the problem of TN-PS, we follow the idea of Li et al. (2022) to specify the neighborhood for a given graph  $G$  in (1). Similar to Alg. 1 in Li et al. (2022), we construct the neighborhood by swapping enumerately two vertices of  $G$ . Suppose the graph  $G$  is of  $N$  vertices, we consequently achieve the neighborhood of  $G$  of the size  $N(N - 1)/2$ .

---

**Algorithm 2** TnALE: the proposed solver of the optimization (1)

---

- 1: **Input:** A solver for the inner minimization of (1); the rank-related radius:  $r_1 \geq r_2 > 0$ ; the number of Iterations in the initialization phase:  $L_0$ ; the number of Iterations in the searching phase:  $L$ ; the number of the round-trips for ALE:  $D$ ;
  - 2: **Initialize:** Uniformly choose a TN structure  $(G, \mathbf{r})$  at random or choose  $(G, \mathbf{r})$  with the specified value;
  - 3: **for**  $l = 1, \dots, L_0$  **do**
  - 4:   Update recursively  $(G, \mathbf{r})$  using Alg. 3 with the center  $(G, \mathbf{r})$ , radius  $r_1$ ,  $D$  round-trips and the loss estimation trick;
  - 5: **end for**
  - 6: **for**  $l = 1, \dots, L$  **do**
  - 7:   Update recursively  $(G, \mathbf{r})$  using Alg. 3 with the center  $(G, \mathbf{r})$ , radius  $r_2$  and  $D$  round-trips ;
  - 8: **end for**
  - 9: **Output:**  $(G, \mathbf{r})$ .
-



## B. Theoretical analysis with proofs

In this section, we first give a rigorous convergence analysis for the algorithms using the local-sampling scheme. After that, we compare the sampling efficiency for TNLS (Li et al., 2022) and the new algorithm.

### B.1. A quick review of tensor network (TN) structure search

Suppose we have the dataset  $D$  and a task-specific loss function  $\pi_D : \mathbb{R}^{I_1 \times I_2 \times \dots \times I_N} \rightarrow \mathbb{R}_+$  associated to  $D$ . The tensor network structure search (TN-SS) problem is to solve the following bi-level optimization problem (Li et al., 2022)

$$\min_{(G, \mathbf{r}) \in \mathbb{G} \times \mathbb{F}_G} \left( \phi(G, \mathbf{r}) + \lambda \cdot \min_{\mathcal{Z} \in \text{TN}S(G, \mathbf{r})} \pi_D(\mathcal{Z}) \right), \quad (8)$$

where  $G \in \mathbb{G}$  is a graph, which owns  $N$  vertices and  $K$  edges and corresponds to the TN-topology,  $\mathbf{r} \in \mathbb{F}_N \subseteq \mathbb{Z}_+^K$  is a positive integer vector of  $K$  dimension corresponding to the TN-ranks,  $\phi : \mathbb{G} \times \mathbb{Z}_+^K \rightarrow \mathbb{R}_+$  represents the function measuring the model complexity of a TN whose structure is modeled by  $(G, \mathbf{r})$ , and  $\lambda > 0$  is a tuning parameter. As expected for TN-SS, solving the problem (8) is intuitively to search for a TN structure modeled by  $(G, \mathbf{r})$ , by which we can give the optimal balance between the complexity and the expressibility of a TN in the task.

We remark that TN-SS can be specified as three sub-problems: *permutation selection (TN-PS, Li et al. (2022))*, *rank selection (TN-RS)* and *topology selection (TN-TS, Li & Sun (2020))*, by specifying the feasible set  $\mathbb{G} \times \mathbb{F}_G$  of (8) into different forms. Specifically, in TN-PS, we set  $\mathbb{F}_G = \mathbb{Z}_+^K$  and  $\mathbb{G}$  is defined as the isomorphic graphs to a ‘‘template’’  $G_0$ , so that only the ranks and vertex permutations are searched while the TN-topology is preserved. In TN-RS, however, we typically restrict the graph  $G$  in (8), i.e.,  $\mathbb{G} = \{G_0\}$  but consider searching for all possible ranks i.e.,  $\mathbb{F}_G = \mathbb{Z}_+^K$ . In TN-TS, we relax  $\mathbb{G}$  to be a set containing all possible simple graphs of order  $N$  and the set  $\mathbb{F}_N$  can be fixed (Li & Sun, 2020) or not (Hashemizadeh et al., 2020). It is known from (Ye & Lim, 2019; Hashemizadeh et al., 2020) that the TN-PS problem with the rank searching can be simplified as a TN-RS problem associated to a ‘‘fully-connected’’ TN (Zheng et al., 2021).

### B.2. Analysis of descent steps

We start the analysis by rewriting (8) into a more general form:

$$\min_{\mathbf{x} \in \mathbb{Z}_+^K, p \in \mathbb{P}} f_p(\mathbf{x}) := f \circ p(\mathbf{x}), \quad (9)$$

where  $\circ$  denotes the function composition,  $f : \mathbb{Z}_{\geq 0}^L \rightarrow \mathbb{R}_+$  is a generalization of the objective function of (8),  $\mathbf{x} \in \mathbb{Z}_+^K$  corresponds to the rank-related variable  $\mathbf{r}$  of (8), and the operator  $p : \mathbb{Z}_+^K \rightarrow \mathbb{Z}_{\geq 0}^L$  and its feasible set  $\mathbb{P}$  correspond to the topology-related variable  $G$  and the set  $\mathbb{G}$  of (8), respectively.

The relationship between  $p \in \mathbb{P}$  of (9) and  $G \in \mathbb{G}$  of (8) is demonstrated as follows. Since in (8) the entries of  $\mathbf{r}$  can be regarded as labels on the edges of  $G$ , the pair  $(G, \mathbf{r})$  can be described as a weighted adjacency matrix of  $N \times N$ . For example, a 4-th order tensor ring (TR, Zhao et al., 2016) of the ranks- $\{2, 3, 4, 5\}$  can be described as

$$(G_1, \mathbf{r}) = \left( \left( \begin{pmatrix} 0 & 0 & 1 & 1 \\ 0 & 0 & 1 & 1 \\ 1 & 1 & 0 & 0 \\ 1 & 1 & 0 & 0 \end{pmatrix}, \begin{pmatrix} 2 \\ 3 \\ 4 \\ 5 \end{pmatrix} \right) \Rightarrow \mathbf{A}_1 = \begin{pmatrix} 0 & 0 & 2 & 3 \\ 0 & 0 & 4 & 5 \\ 2 & 3 & 0 & 0 \\ 4 & 5 & 0 & 0 \end{pmatrix}, \quad (10)$$

or

$$(G_2, \mathbf{r}) = \left( \left( \begin{pmatrix} 0 & 1 & 0 & 1 \\ 1 & 0 & 1 & 0 \\ 0 & 1 & 0 & 1 \\ 1 & 0 & 1 & 0 \end{pmatrix}, \begin{pmatrix} 2 \\ 3 \\ 4 \\ 5 \end{pmatrix} \right) \Rightarrow \mathbf{A}_2 = \begin{pmatrix} 0 & 2 & 0 & 5 \\ 2 & 0 & 3 & 0 \\ 0 & 3 & 0 & 4 \\ 5 & 0 & 4 & 0 \end{pmatrix}. \quad (11)$$

Here  $G_1$  and  $G_2$  correspond to the TR topology with different permutations of vertices. In the settings of TN-PS (Li et al., 2022), we can prove that such the relationship is bijective. The operator  $p$  is thus to map the TN-ranks, denoted  $\mathbf{x} \in \mathbb{Z}_+^K$  in (9), onto the vectorization of entries in the upper triangle part (except for the diagonal) of the adjacency matrix. For

example,

$$\mathbf{A}_1 = \begin{pmatrix} 0 & 0 & 2 & 3 \\ 0 & 0 & 4 & 5 \\ 2 & 3 & 0 & 0 \\ 4 & 5 & 0 & 0 \end{pmatrix} \iff p_1(\mathbf{x}) = \begin{pmatrix} 0 & 0 & 0 & 0 \\ 1 & 0 & 0 & 0 \\ 0 & 1 & 0 & 0 \\ 0 & 0 & 1 & 0 \\ 0 & 0 & 0 & 1 \\ 0 & 0 & 0 & 0 \end{pmatrix} \begin{pmatrix} 2 \\ 3 \\ 4 \\ 5 \end{pmatrix} = \begin{pmatrix} 0 \\ 2 \\ 3 \\ 4 \\ 5 \\ 0 \end{pmatrix}, \quad (12)$$

and

$$\mathbf{A}_2 = \begin{pmatrix} 0 & 2 & 0 & 5 \\ 2 & 0 & 3 & 0 \\ 0 & 3 & 0 & 4 \\ 5 & 0 & 4 & 0 \end{pmatrix} \iff p_2(\mathbf{x}) = \begin{pmatrix} 1 & 0 & 0 & 0 \\ 0 & 0 & 0 & 0 \\ 0 & 0 & 0 & 1 \\ 0 & 1 & 0 & 0 \\ 0 & 0 & 0 & 0 \\ 0 & 0 & 1 & 0 \end{pmatrix} \begin{pmatrix} 2 \\ 3 \\ 4 \\ 5 \end{pmatrix} = \begin{pmatrix} 2 \\ 0 \\ 5 \\ 3 \\ 0 \\ 4 \end{pmatrix}. \quad (13)$$

It is shown that  $p$  is essentially an operator produced by the permutation padding with several rows of zeros according to  $G$ .

The convergence analysis of this work is mainly inspired by Golovin et al. (2019), which establishes a convex framework for the gradient-less optimization algorithms in the real domain. The challenge is, the TN-SS problem is essentially discrete, so that many well-developed tools, such as convexity and smoothness, for convergence analysis turn invalid in the discrete scenario.

To bridge the graph from Golovin et al. (2019) to TN-SS, we first re-define several important concepts, by which the necessary tools for the analysis are re-derived. In doing so, we begin by introducing the finite gradient as the alternative to the classic one defined in the continuous domain.

**Definition B.1 (finite gradient).** For any function  $f : \mathbb{Z}_{\geq 0}^L \rightarrow \mathbb{R}$ , its finite gradient  $\Delta f : \mathbb{Z}_{\geq 0}^L \rightarrow \mathbb{R}^L$  at the point  $\mathbf{x}$  is defined as the vector

$$\Delta f(\mathbf{x}) = [f(\mathbf{x} + \mathbf{e}_1) - f(\mathbf{x}), \dots, f(\mathbf{x} + \mathbf{e}_L) - f(\mathbf{x})]^\top, \quad (14)$$

where  $\mathbf{e}_i \forall i \in [L]$  denote the unit vectors with the  $i$ -th entry being one and other entries being zeros.

Applying the finite gradient defined in (14), we also re-define the strong convexity and smoothness for analysis in the discrete domain.

**Definition B.2 ( $\alpha$ -strong convexity with finite gradient).** We say  $f$  is  $\alpha$ -strongly convex for  $\alpha \geq 0$  if  $f(\mathbf{y}) \geq f(\mathbf{x}) + \langle \Delta f(\mathbf{x}) - \frac{\alpha}{2} \mathbf{1}, \mathbf{y} - \mathbf{x} \rangle + \frac{\alpha}{2} \|\mathbf{y} - \mathbf{x}\|^2$  for all  $\mathbf{x}, \mathbf{y} \in \mathbb{Z}_{\geq 0}^L$ , where  $\mathbf{1} \in \mathbb{R}^L$  denotes the vector with all entries being one. We simply say  $f$  is convex if it is  $\alpha$ -strongly convex and  $\alpha = 0$ .

Compared to the definitions used in Golovin et al. (2019) and other literature for convex analysis, the additional term,  $\frac{\alpha}{2} \mathbf{1}$ , marked by the *blue* color, appears due to the discrepancy of the finite gradient and its counterpart in the continuous domain. Below, we prove several basic results using the  $\alpha$ -strong convexity with finite gradient.

**Lemma B.3.** *If  $f$  is  $\alpha$ -strongly convex in  $\mathbb{Z}_{\geq 0}^L$ , then the following inequalities are held:*

1.  $g(\mathbf{x}) = f(\mathbf{x}) - \frac{\alpha}{2} \|\mathbf{x}\|^2$  is convex in the discrete scenario for all  $\mathbf{x} \in \mathbb{Z}_{\geq 0}^L$ , and vice versa;
2.  $\langle \Delta f(\mathbf{x}) - \Delta f(\mathbf{y}), \mathbf{x} - \mathbf{y} \rangle \geq \alpha \|\mathbf{x} - \mathbf{y}\|^2$  for any  $\mathbf{x}, \mathbf{y} \in \mathbb{Z}_{\geq 0}^L$ ;
3.  $\|\Delta f(\mathbf{x}) - \Delta f(\mathbf{y})\| \geq \alpha \|\mathbf{x} - \mathbf{y}\|$  for any  $\mathbf{x}, \mathbf{y} \in \mathbb{Z}_{\geq 0}^L$ ;

Here  $\|\cdot\|$  denotes the  $l_2$  norm for vectors.

*Proof.* (1,  $\Rightarrow$ ) According to Def. B.2, the first statement is equivalent to proving the inequality

$$g(\mathbf{y}) \geq g(\mathbf{x}) + \langle \Delta g(\mathbf{x}), \mathbf{y} - \mathbf{x} \rangle \quad (15)$$

holding for any  $\mathbf{x}, \mathbf{y} \in \mathbb{Z}_{\geq 0}^L$ . Applying the  $\alpha$ -strong convexity assumption, it follows that

$$\begin{aligned}
 g(\mathbf{y}) - g(\mathbf{x}) - \langle \Delta g(\mathbf{x}), \mathbf{y} - \mathbf{x} \rangle &= f(\mathbf{y}) - \frac{\alpha}{2} \|\mathbf{y}\|^2 - f(\mathbf{x}) + \frac{\alpha}{2} \|\mathbf{x}\|^2 - \langle \Delta g(\mathbf{x}), \mathbf{y} - \mathbf{x} \rangle \\
 &= f(\mathbf{y}) - \frac{\alpha}{2} \|\mathbf{y}\|^2 - f(\mathbf{x}) + \frac{\alpha}{2} \|\mathbf{x}\|^2 - \left\langle \Delta f(\mathbf{x}) - \frac{\alpha}{2} (2\mathbf{x} + \mathbf{1}), \mathbf{y} - \mathbf{x} \right\rangle \\
 &= f(\mathbf{y}) - f(\mathbf{x}) - \left\langle \Delta f(\mathbf{x}) - \frac{\alpha}{2} \mathbf{1}, \mathbf{y} - \mathbf{x} \right\rangle - \frac{\alpha}{2} \|\mathbf{y}\|^2 + \frac{\alpha}{2} \|\mathbf{x}\|^2 + \frac{\alpha}{2} \langle 2\mathbf{x}, \mathbf{y} - \mathbf{x} \rangle \\
 &\geq \frac{\alpha}{2} (\|\mathbf{y} - \mathbf{x}\|^2 - \|\mathbf{y}\|^2 - \|\mathbf{x}\|^2 + 2 \langle \mathbf{x}, \mathbf{y} \rangle) = 0.
 \end{aligned} \tag{16}$$

Here the first equality follows from the definition of  $g(\mathbf{x})$ , the second equality holds since the finite gradient  $\Delta \|\mathbf{x}\|^2 = 2\mathbf{x} + \mathbf{1}$ , and the inequality at the bottom line follows from the  $\alpha$ -strong convexity assumption on  $f$ .

(1,  $\Leftarrow$ ) By (15),

$$f(\mathbf{y}) - \frac{\alpha}{2} \|\mathbf{y}\|^2 \geq f(\mathbf{x}) - \frac{\alpha}{2} \|\mathbf{x}\|^2 + \left\langle \Delta f(\mathbf{x}) - \frac{\alpha}{2} (2\mathbf{x} + \mathbf{1}), \mathbf{y} - \mathbf{x} \right\rangle. \tag{17}$$

The  $\alpha$ -strong convexity of  $f$  is thus proved by algebraically simplifying (17).

(2) To prove the second statement, we first know that the following inequality

$$\langle \Delta g(\mathbf{x}) - \Delta g(\mathbf{y}), \mathbf{x} - \mathbf{y} \rangle \geq 0, \quad \forall \mathbf{x}, \mathbf{y} \tag{18}$$

holds since the monotone gradient property of the convexity (it is true in both continuous and discrete scenarios). By the form of  $\Delta g(\mathbf{x})$ , it follows that

$$\left\langle \Delta f(\mathbf{x}) - \frac{\alpha}{2} (2\mathbf{x} + \mathbf{1}) - \Delta f(\mathbf{y}) + \frac{\alpha}{2} (2\mathbf{y} + \mathbf{1}), \mathbf{x} - \mathbf{y} \right\rangle \geq 0. \tag{19}$$

With algebraic simplification, we obtain

$$\langle \Delta f(\mathbf{x}) - \Delta f(\mathbf{y}), \mathbf{x} - \mathbf{y} \rangle \geq \alpha \|\mathbf{x} - \mathbf{y}\|^2 \tag{20}$$

for all  $\mathbf{x}, \mathbf{y} \in \mathbb{Z}_{\geq 0}^L$ . The second statement is thus proved.

(3) The third statement holds since the following relationship

$$\|\Delta f(\mathbf{x}) - \Delta f(\mathbf{y})\| \|\mathbf{x} - \mathbf{y}\| \geq \langle \Delta f(\mathbf{x}) - \Delta f(\mathbf{y}), \mathbf{x} - \mathbf{y} \rangle \geq \alpha \|\mathbf{x} - \mathbf{y}\|^2, \tag{21}$$

where the first inequality follows from the Cauchy–Schwarz inequality, and the second inequality follows from (20). The third statement is proved by dividing by  $\|\mathbf{x} - \mathbf{y}\|$  on both sides.  $\square$

Apart from the convexity, the smoothness of the objective function is also required to be re-defined in the discrete scenario.

**Definition B.4** ( $(\beta_1, \beta_2)$ -smoothness with finite gradient). We say  $f$  is  $(\beta_1, \beta_2)$ -smooth for  $\beta_1, \beta_2 > 0$  if

1.  $|f(\mathbf{x}) - f(\mathbf{y})| \leq \beta_1 \|\mathbf{x} - \mathbf{y}\|$  for all  $\mathbf{x}, \mathbf{y} \in \mathbb{Z}_{\geq 0}^L$ ;
2. The function  $l(\mathbf{x}) := \frac{\beta_2}{2} \|\mathbf{x}\|^2 - f(\mathbf{x})$  is convex.

The first item of Def. B.4 restricts that  $f$  is  $\beta_1$ -Lipschitz, implying the ‘‘continuity’’ of the function, while the second item upper bounds the change of the finite gradient of  $f$ , implying a ‘‘continuity’’ over the finite gradient. In particular,

**Lemma B.5.** *If  $l(\mathbf{x}) = \frac{\beta_2}{2} \|\mathbf{x}\|^2 - f(\mathbf{x})$  is convex, then for all  $\mathbf{x}, \mathbf{y} \in \mathbb{Z}_{\geq 0}^L$*

1.  $f(\mathbf{y}) \leq f(\mathbf{x}) + \left\langle \Delta f(\mathbf{x}) - \frac{\beta_2}{2} \mathbf{1}, \mathbf{y} - \mathbf{x} \right\rangle + \frac{\beta_2}{2} \|\mathbf{y} - \mathbf{x}\|^2$  and vice versa;
2.  $\langle \Delta f(\mathbf{x}) - \Delta f(\mathbf{y}), \mathbf{x} - \mathbf{y} \rangle \leq \beta \|\mathbf{x} - \mathbf{y}\|^2$ .

*Proof.* (1,  $\Rightarrow$ ) By the form  $l(\mathbf{x})$  and its convex property, we have the inequality

$$\frac{\beta}{2}\|\mathbf{y}\|^2 - f(\mathbf{y}) \geq \frac{\beta}{2}\|\mathbf{x}\|^2 - f(\mathbf{x}) + \left\langle \frac{\beta}{2}(2\mathbf{x} + \mathbf{1}) - \Delta f(\mathbf{x}), \mathbf{y} - \mathbf{x} \right\rangle. \quad (22)$$

The first statement is proved by algebraically simplifying (22). The ( $\Leftarrow$ ) direction can be proved similarly.

To prove the second item, by the convexity of  $l(\mathbf{x})$ ,

$$l(\mathbf{y}) \geq l(\mathbf{x}) + \langle \Delta l(\mathbf{x}), \mathbf{y} - \mathbf{x} \rangle. \quad (23)$$

Similarly,

$$l(\mathbf{x}) \geq l(\mathbf{y}) + \langle \Delta l(\mathbf{y}), \mathbf{x} - \mathbf{y} \rangle. \quad (24)$$

Summing the two sides of (23) and (24) up, we have

$$\langle \Delta l(\mathbf{x}) - \Delta l(\mathbf{y}), \mathbf{x} - \mathbf{y} \rangle \geq 0. \quad (25)$$

Applying  $l(\mathbf{x}) = \frac{\beta}{2}\|\mathbf{x}\|^2 - f(\mathbf{x})$ ,

$$\langle \beta(2\mathbf{x} + \mathbf{1}) - \Delta f(\mathbf{x}) - \beta(2\mathbf{y} + \mathbf{1}) + \Delta f(\mathbf{y}), \mathbf{x} - \mathbf{y} \rangle \geq 0. \quad (26)$$

By simplifying the inequality, we finally have

$$\langle \Delta f(\mathbf{x}) - \Delta f(\mathbf{y}), \mathbf{x} - \mathbf{y} \rangle \leq \beta\|\mathbf{x} - \mathbf{y}\|^2. \quad (27)$$

□

The first item of Def. B.4 gives the following crucial result, which is used in the main theorem of this paper.

**Lemma B.6.** *If  $|f(\mathbf{x}) - f(\mathbf{y})| \leq \beta\|\mathbf{x} - \mathbf{y}\|$  for all  $\mathbf{x}, \mathbf{y} \in \mathbb{Z}_{\geq 0}^L$ , then the norm of the finite gradient with respect to  $\mathbf{x}$  is bounded, i.e.,  $\|\Delta f(\mathbf{x})\|_{\infty} \leq \beta$ .*

*Proof.* Denote  $\Delta f(\mathbf{x})_i$  the  $i$ -th entry of  $\Delta f(\mathbf{x})$ , then for all  $1 \leq i \leq L$  the second item of the definition follows by

$$|\Delta f(\mathbf{x})_i| = |f(\mathbf{x} + \mathbf{e}_i) - f(\mathbf{x})| \leq \beta\|\mathbf{x} + \mathbf{e}_i - \mathbf{x}\| = \beta, \quad (28)$$

where  $\mathbf{e}_i$  denotes the unit vector with  $i$ -th entry being one and others being zeros, and the first equality follows from the definition of the finite gradient. □

After the new definitions of convexity and smoothness with finite gradient, in the proof, we also use the concept of the sub-level set, which is widely used in optimization theory. For the self-consistency purpose, the specific definition is reviewed as follows:

**Definition B.7 (sub-level set).** The level set of  $f$  at point  $\mathbf{x} \in \mathbb{Z}_{\geq 0}^L$  is  $\mathbb{L}_{\mathbf{x}}(f) = \{\mathbf{y} \in \mathbb{Z}_{\geq 0}^L : f(\mathbf{y}) = f(\mathbf{x})\}$ . The sub-level set of  $f$  at point  $\mathbf{x} \in \mathbb{Z}_{\geq 0}^L$  is  $\mathbb{L}_{\mathbf{x}}^{\downarrow}(f) = \{\mathbf{y} \in \mathbb{Z}_{\geq 0}^L : f(\mathbf{y}) \leq f(\mathbf{x})\}$ .

The following lemma shows that, for any  $\mathbf{x}$ , there exists a cube, i.e., a ball with infinity-norm, which is tangent at  $\mathbf{x}$  and inside the sub-level set  $\mathbb{L}_{\mathbf{x}}^{\downarrow}(f)$ .

**Lemma B.8 (the sub-level cube).** *Assume that  $f : \mathbb{Z}_{\geq 0}^L \rightarrow \mathbb{R}$  is  $\alpha$ -strongly convex,  $(\beta_1, \beta_2)$ -smooth, and its minimum, denoted  $f(\mathbf{x}^*)$ , satisfies  $\|\frac{\beta_2}{2}\mathbf{1} - \Delta f(\mathbf{x}^*)\| \leq \gamma$  where  $\gamma$  is a constant and  $0 \leq \gamma < \alpha$ . Then, for all  $\mathbf{x} \in \mathbb{Z}_{\geq 0}^L$ , there is a  $L$ -dimensional cube, which is of the edge length  $\frac{2(\alpha-\gamma)}{\beta_2\sqrt{L}}\|\mathbf{x} - \mathbf{x}^*\|$ , tangent at  $\mathbf{x}$ , and inside the sub-level set  $\mathbb{L}_{\mathbf{x}}^{\downarrow}(f)$ .*

*Proof.* Applying the smoothness assumption and Lemma B.5,

$$\begin{aligned} f\left(\mathbf{x} - \frac{1}{\beta_2}\Delta f(\mathbf{x}) + \frac{1}{2}\mathbf{1} + \mathbf{s}\right) &\leq f(\mathbf{x}) + \left\langle \Delta f(\mathbf{x}) - \frac{\beta_2}{2}\mathbf{1}, \mathbf{s} + \frac{1}{2}\mathbf{1} - \frac{1}{\beta_2}\Delta f(\mathbf{x}) \right\rangle + \frac{\beta_2}{2}\left\|\mathbf{s} + \frac{1}{2}\mathbf{1} - \frac{1}{\beta_2}\Delta f(\mathbf{x})\right\|^2 \\ &= f(\mathbf{x}) + \frac{\beta_2}{2}\left(\|\mathbf{s}\|^2 - \left\|\frac{1}{2}\mathbf{1} - \frac{1}{\beta_2}\Delta f(\mathbf{x})\right\|^2\right) \end{aligned} \quad (29)$$

for any  $\mathbf{s}$ . The inequality (29) implies that for any  $\mathbf{y} \in \mathbb{Z}_{\geq 0}^L$  in the Euclidean ball  $B\left(\mathbf{x} - \frac{1}{\beta_2} \Delta f(\mathbf{x}) + \frac{1}{2} \mathbf{1}, \left\| \frac{1}{2} \mathbf{1} - \frac{1}{\beta_2} \Delta f(\mathbf{x}) \right\| \right)$  it yields  $f(\mathbf{y}) \leq f(\mathbf{x})$ , *i.e.*,  $\mathbf{y} \in \mathbb{L}_{\mathbf{x}}^{\downarrow}(f)$ . We also see that  $\mathbf{x}$  is at the surface of this Euclidean ball, *i.e.*, the ball is tangent at  $\mathbf{x}$ . Furthermore, we also prove that the radius of the ball is lower bounded as follows:

$$\begin{aligned} \frac{1}{\beta_2} \left\| \frac{\beta_2}{2} \mathbf{1} - \Delta f(\mathbf{x}) \right\| &= \frac{1}{\beta_2} \left\| \frac{\beta_2}{2} \mathbf{1} - \Delta f(\mathbf{x}^*) + \Delta f(\mathbf{x}^*) - \Delta f(\mathbf{x}) \right\| \\ &\geq \frac{1}{\beta_2} \left( \left\| \Delta f(\mathbf{x}) - \Delta f(\mathbf{x}^*) \right\| - \left\| \frac{\beta_2}{2} \mathbf{1} - \Delta f(\mathbf{x}^*) \right\| \right) \\ &\geq \frac{(\alpha - \gamma)}{\beta_2} \|\mathbf{x} - \mathbf{x}^*\|, \end{aligned} \quad (30)$$

where the inequality at the bottom line follows from the third statement of Lemma B.3 and the assumption  $\left\| \frac{\beta_2}{2} \mathbf{1} - \Delta f(\mathbf{x}^*) \right\| \leq \gamma$ .

Next, we show that the ball  $B\left(\mathbf{x} - \frac{1}{\beta_2} \Delta f(\mathbf{x}) + \frac{1}{2} \mathbf{1}, \left\| \frac{1}{2} \mathbf{1} - \frac{1}{\beta_2} \Delta f(\mathbf{x}) \right\| \right)$  contains a cube of edge length  $\frac{2(\alpha - \gamma)}{\beta_2 \sqrt{L}} \|\mathbf{x} - \mathbf{x}^*\|$ . First, we easily know in the ball there exists a cube, of which the volume is sufficiently small, and one vertex is at  $\mathbf{x}$ . Then, the cube gradually extends all edges until the adjacent vertices of  $\mathbf{x}$  touch the surface of the ball. At this moment, it can be seen that the edges that touch the surface of the ball turn the chords of the ball. Furthermore, the line connecting the ball center to  $\mathbf{x}$  has an equal angle to all edges connecting  $\mathbf{x}$ , due to the symmetry of the geometrical shapes. With basic geometry knowledge, we can thus calculate the chord length, *i.e.*, the edge length of the cube, with  $2 \times R \cos(\theta)$ , where  $R$  denotes the radius of the ball and  $\theta = \arccos(1/\sqrt{L})$  is the angle between the chord and the "center- $\mathbf{x}$ " line. Finally, using (30), we know the cube of the edge length  $\frac{2(\alpha - \gamma)}{\beta_2 \sqrt{L}} \|\mathbf{x} - \mathbf{x}^*\|$  is tangent at  $\mathbf{x}$ , and inside sub-level set  $\mathbb{L}_{\mathbf{x}}^{\downarrow}(f)$ .  $\square$

**Lemma B.9 (convex combination in the discrete domain).** *Suppose  $\mathbf{q} = \theta \mathbf{x} + (1 - \theta) \mathbf{y}$ ,  $\forall \theta \in [0, 1]$ , and there is  $\hat{\mathbf{q}} \in \mathbb{Z}_{\geq 0}^L$  where  $\mathbf{\Lambda} = \mathbf{q} - \hat{\mathbf{q}}$ . If  $f$  is  $\alpha$ -strongly convex, then*

$$\theta f(\mathbf{x}) + (1 - \theta) f(\mathbf{y}) \geq f(\hat{\mathbf{q}}) + \left\langle \Delta f(\hat{\mathbf{q}}) - \frac{\alpha}{2} \mathbf{1}, \mathbf{\Lambda} \right\rangle + \frac{\alpha}{2} \|\mathbf{\Lambda}\|^2. \quad (31)$$

*Proof.* By the definition of the  $\alpha$ -strong convexity,

$$\begin{aligned} f(\mathbf{x}) &\geq f(\hat{\mathbf{q}}) + \left\langle \Delta f(\hat{\mathbf{q}}) - \frac{\alpha}{2} \mathbf{1}, \mathbf{x} - \hat{\mathbf{q}} \right\rangle + \frac{\alpha}{2} \|\mathbf{x} - \hat{\mathbf{q}}\|^2; \\ f(\mathbf{y}) &\geq f(\hat{\mathbf{q}}) + \left\langle \Delta f(\hat{\mathbf{q}}) - \frac{\alpha}{2} \mathbf{1}, \mathbf{y} - \hat{\mathbf{q}} \right\rangle + \frac{\alpha}{2} \|\mathbf{y} - \hat{\mathbf{q}}\|^2. \end{aligned} \quad (32)$$

Thus, we have their convex combination as

$$\begin{aligned} \theta f(\mathbf{x}) + (1 - \theta) f(\mathbf{y}) &\geq f(\hat{\mathbf{q}}) + \left\langle \Delta f(\hat{\mathbf{q}}) - \frac{\alpha}{2} \mathbf{1}, \mathbf{\Lambda} \right\rangle + \frac{\alpha}{2} (\theta \|\mathbf{x}\|^2 + (1 - \theta) \|\mathbf{y}\|^2 + \|\hat{\mathbf{q}}\|^2 - 2 \langle \mathbf{q}, \hat{\mathbf{q}} \rangle) \\ &\geq f(\hat{\mathbf{q}}) + \left\langle \Delta f(\hat{\mathbf{q}}) - \frac{\alpha}{2} \mathbf{1}, \mathbf{\Lambda} \right\rangle + \frac{\alpha}{2} (\|\mathbf{q}\|^2 + \|\hat{\mathbf{q}}\|^2 - 2 \langle \mathbf{q}, \hat{\mathbf{q}} \rangle), \\ &= f(\hat{\mathbf{q}}) + \left\langle \Delta f(\hat{\mathbf{q}}) - \frac{\alpha}{2} \mathbf{1}, \mathbf{\Lambda} \right\rangle + \frac{\alpha}{2} \|\mathbf{\Lambda}\|^2 \end{aligned} \quad (33)$$

where the second inequality follows from the convexity of  $\|\cdot\|^2$ . The proof is completed.  $\square$

**Assumption B.10.** Assume that  $f : \mathbb{Z}_{\geq 0}^L \rightarrow \mathbb{R}_+$  of (9) is  $\alpha$ -strongly convex,  $(\beta_1, \beta_2)$ -smooth, and its minimum, denoted  $(p^*, \mathbf{x}^*) = \arg \min_{p, \mathbf{x}} f \circ p(\mathbf{x})$ , satisfies  $\|\Delta f_{p^*}(\mathbf{x}^*) - \frac{\beta_2}{2} \mathbf{1}\| \leq \gamma$  where  $0 \leq \gamma < \alpha \leq \beta_1 \leq \beta_2 \leq 1$ .

Here the inequality  $\|\Delta f_{p^*}(\mathbf{x}^*) - \frac{\beta_2}{2} \mathbf{1}\| \leq \gamma$  implies that, up to a (small) constant vector  $\frac{\beta_2}{2} \mathbf{1}$ , the finite gradient at  $(p^*, \mathbf{x}^*)$  should be sufficiently small, which can be understood as the discrete version of the zero-gradient for the stationary points in the continuous domain. The upper bound "1" is arbitrarily chosen just for simplifying the calculation. Also note that  $\beta_2$  must be larger than  $\alpha$  due to the fact  $\alpha \|\mathbf{x} - \mathbf{y}\|^2 \leq \langle \Delta f(\mathbf{x}) - \Delta f(\mathbf{y}), \mathbf{x} - \mathbf{y} \rangle \leq \beta_2 \|\mathbf{x} - \mathbf{y}\|^2$  (see Lemma B.3 and Lemma B.5). With Assumption B.10, we next prove that the local-sampling-based searching algorithm achieves the linear convergence rate up to a constant, *if  $p^*$  is known beforehand.*

**Theorem B.11 (convergence rate).** *Suppose Assumption B.10 is satisfied, the operator  $p$  in (9) is fixed to be  $p^*$ , and  $0 \leq \theta \leq 1$ . Then, for any  $\mathbf{x}$  with  $\|\mathbf{x} - \mathbf{x}^*\|_\infty \leq c$ , we can find a neighborhood  $B_\infty(\mathbf{x}, r_x)$  where  $r_x \geq \theta c + \frac{1}{2}$ , such that there exist a element  $\mathbf{y} \in B_\infty(\mathbf{x}, r_x)$  satisfying*

$$f_{p^*}(\mathbf{y}) - f_{p^*}(\mathbf{x}^*) \leq (1 - \theta)(f_{p^*}(\mathbf{x}) - f_{p^*}(\mathbf{x}^*)) + \frac{7}{8}K. \quad (34)$$

*Proof.* First of all, since the operator  $p$  is fixed to be  $p^*$ , the problem (9) can be equivalently simplified by removing the formulation of  $p$  out of (9), which is written as

$$\min_{\mathbf{x} \in \mathbb{Z}_+^K} f(\mathbf{x}), \quad (35)$$

where  $f : \mathbb{Z}_{\geq 0}^K \rightarrow \mathbb{R}$  represents the objective function.<sup>6</sup> By Lemma B.9, we have the following inequality:

$$f(\hat{\mathbf{q}}) - f(\mathbf{x}^*) \leq (1 - \theta)(f(\mathbf{x}) - f(\mathbf{x}^*)) + \left\langle \frac{\alpha}{2} \mathbf{1} - \Delta f(\hat{\mathbf{q}}), \mathbf{\Lambda} \right\rangle - \frac{\alpha}{2} \|\mathbf{\Lambda}\|^2. \quad (36)$$

Next, we prove in the neighborhood  $B(\mathbf{x}, r_x)$  there exists an element  $\mathbf{y}$ , which belongs to as well the sub-level cube tangent at  $\hat{\mathbf{q}}$  knowing by Lemma B.8, so that  $f(\mathbf{y}) \leq f(\hat{\mathbf{q}})$  holds. To do so, we first know that the distance between  $\hat{\mathbf{q}}$  and  $p_x(\mathbf{x})$  satisfying

$$\|\mathbf{x} - \hat{\mathbf{q}}\|_\infty = \|\mathbf{x} - \mathbf{q} + \mathbf{\Lambda}\|_\infty \leq \|\mathbf{x} - \mathbf{q}\|_\infty + \|\mathbf{\Lambda}\|_\infty = \theta \|\mathbf{x} - \mathbf{x}^*\|_\infty + \|\mathbf{\Lambda}\|_\infty \leq \theta c + \frac{1}{2}. \quad (37)$$

Here the last inequality follows from  $\|\mathbf{\Lambda}\|_\infty \leq \frac{1}{2}$ , which holds because  $\hat{\mathbf{q}} \in \mathbb{Z}_{\geq 0}^K$  can be always found by rounding the entries of  $\mathbf{q}$  into the closest integers. We thus know from the inequality that the intersection between the sub-level cube tangent at  $\hat{\mathbf{q}}$  and  $B(\mathbf{x}, r_x)$  is not empty if  $r_x \geq \theta c + \frac{1}{2}$ , proving the existence of the  $\mathbf{y}$ . Last, we bound (36) as follows:

$$\begin{aligned} f(\mathbf{y}) - f(\mathbf{x}^*) &\leq f(\hat{\mathbf{q}}) - f(\mathbf{x}^*) \leq (1 - \theta)(f(\mathbf{x}) - f(\mathbf{x}^*)) + \left\langle \frac{\alpha}{2} \mathbf{1} - \Delta f(\hat{\mathbf{q}}), \mathbf{\Lambda} \right\rangle - \frac{\alpha}{2} \|\mathbf{\Lambda}\|^2 \\ &\leq (1 - \theta)(f(\mathbf{x}) - f(\mathbf{x}^*)) + \left| \left\langle \frac{\alpha}{2} \mathbf{1}, \mathbf{\Lambda} \right\rangle \right| + |\langle \Delta f(\hat{\mathbf{q}}), \mathbf{\Lambda} \rangle| + \frac{\alpha}{2} \|\mathbf{\Lambda}\|^2 \\ &\leq (1 - \theta)(f(\mathbf{x}) - f(\mathbf{x}^*)) + \frac{\alpha}{4} K + \|\Delta f(\hat{\mathbf{q}})\|_\infty \|\mathbf{\Lambda}\|_1 + \frac{\alpha}{2} \|\mathbf{\Lambda}\|^2 \\ &\leq (1 - \theta)(f(\mathbf{x}) - f(\mathbf{x}^*)) + \frac{\alpha}{4} K + \frac{\beta_1}{2} K + \frac{\alpha}{8} K \\ &\leq (1 - \theta)(f(\mathbf{x}) - f(\mathbf{x}^*)) + \frac{3\alpha + 4\beta_1}{8} K \\ &\leq (1 - \theta)(f(\mathbf{x}) - f(\mathbf{x}^*)) + \frac{7}{8} K. \end{aligned} \quad (38)$$

Here the inequality in the fourth line follows from Lemma B.6 and  $\|\mathbf{\Lambda}\|_\infty \leq 1/2$ , and the inequality at the bottom line follows from Assumption B.10 that  $\alpha < \beta_1 \leq 1$ . The proof is thus completed.  $\square$

It is known from the proof that the constant  $(7/8)K$  appearing in (34) is due to the fact  $\|\mathbf{\Lambda}\|_1 \leq K\|\mathbf{\Lambda}\|_\infty \leq K/2$  and  $\|\mathbf{\Lambda}\|_2 \leq K\|\mathbf{\Lambda}\|_\infty \leq \sqrt{K}/2$ . It means that with the rounding error  $\|\mathbf{\Lambda}\|_\infty \leq 1/2$ , the  $l_{1,2}$  norm of  $\mathbf{\Lambda}$  would become larger with increasing the dimension  $K$ , which is inevitable in the analysis. It only disappears if  $\|\mathbf{\Lambda}\|_\infty = 0$ , implying the conventional convex optimization in the continuous domain.

As an important corollary from Theorem B.11, we next prove the convergence guarantee for the local-sampling-based methods.

**Corollary B.12 (convergence guarantee).** *Suppose  $p^*$  is known and a series  $\{\mathbf{x}_n\}_{n=0}^\infty$ , where  $\mathbf{x}_0$  is randomly chosen in  $\mathbb{Z}_+^K$ , and for each  $n > 0$ ,  $\mathbf{x}_n$  is equal to the  $\mathbf{y}$  in Theorem B.11. Then we can achieve the following limit when  $\Omega(1/K) \leq \theta \leq 1$ ,*

$$\lim_{n \rightarrow \infty} (f_{p^*}(\mathbf{x}_n) - f_{p^*}(\mathbf{x}^*)) = O(1) \quad (39)$$

<sup>6</sup>Here for brevity, we re-use the notation of  $f$  without ambiguity since the main properties of  $f$  are preserved up to the domain restricting from  $\mathbb{Z}_{\geq 0}^L$  to  $\mathbb{Z}_{\geq 0}^K$ .

*Proof.* Let  $C_K := (7/8)K$ . By the updating rule,

$$\begin{aligned}
 f_{p^*}(\mathbf{x}_n) - f_{p^*}(\mathbf{x}^*) &\leq (1 - \theta)(f_{p^*}(\mathbf{x}_{n-1}) - f_{p^*}(\mathbf{x}^*)) + C_K \\
 &\leq (1 - \theta)^2(f_{p^*}(\mathbf{x}_{n-2}) - f_{p^*}(\mathbf{x}^*)) + C_K + C_K(1 - \theta) \\
 &\leq (1 - \theta)^3(f_{p^*}(\mathbf{x}_{n-3}) - f_{p^*}(\mathbf{x}^*)) + C_K + C_K(1 - \theta) + C_K(1 - \theta)^2 \\
 &\leq \dots \\
 &\leq (1 - \theta)^n(f_{p^*}(\mathbf{x}_0) - f_{p^*}(\mathbf{x}^*)) + C_K \sum_{m=1}^n (1 - \theta)^{m-1}.
 \end{aligned} \tag{40}$$

Thus using the condition  $\Omega(1/K) \leq \theta \leq 1$ , we finally obtain that

$$\lim_{n \rightarrow \infty} (f_{p^*}(\mathbf{x}_n) - f_{p^*}(\mathbf{x}^*)) \leq 0 + C_K \frac{1}{\theta} = O(1). \tag{41}$$

□

### B.3. Sampling efficiency

**Proposition B.13 (curse of dimensionality for TNLS).** *Let the assumptions in Theorem B.11 be satisfied. Furthermore, assume that  $\mathbf{x}^*$  is sufficiently smaller (or larger) than  $\mathbf{x}$  entry-wisely except for a constant number of entries. Then the probability of achieving a suitable  $\mathbf{y}$  as mentioned in Theorem B.11 by uniformly randomly sampling in  $B_\infty(\mathbf{x}, r_{\mathbf{x}})$  with  $r_{\mathbf{x}} \geq \theta c + \frac{1}{2}$  equals  $O(2^{-K})$ .*

*Proof.* We only prove the case where  $\mathbf{x}^*$  is sufficiently smaller than  $\mathbf{x}$  in the entry-wise manner, except a constant number of entries. The ‘‘larger’’ case can be proved similarly. Recall Theorem B.11. By the construction of  $\mathbf{y}$ , we have  $\mathbf{q} = \theta \mathbf{x} + (1 - \theta)\mathbf{x}^*$  with  $0 \leq \theta \leq 1$  and the approximation  $\hat{\mathbf{q}} \in \mathbb{Z}_+^K$  with  $\hat{\mathbf{q}} = \mathbf{q} + \mathbf{\Lambda}$  and  $\|\mathbf{\Lambda}\|_\infty \leq 1/2$ . According to the assumptions, we know  $\mathbf{x} - \hat{\mathbf{q}}$  is entry-wisely larger than zero except  $C$  entries, where  $C \geq 0$  is a constant. Since  $r_{\mathbf{x}} \geq \theta c + \frac{1}{2}$ , we further know from Theorem B.11 that the intersection between  $B_\infty(x, r_{\mathbf{x}})$ , denoted  $B$  in the rest of the proof for brevity, and the sub-level cube, denoted  $A$ , tangent at  $\hat{\mathbf{q}}$  is not empty. In this case, we can easily bound the volume of the cube associated to the intersection of  $A$  and  $B$  as follows:

$$|A \cap B| \leq (r_{\mathbf{x}} - \delta_{\min})^{K-C} (r_{\mathbf{x}} + \delta_{\max})^C. \tag{42}$$

Here  $|\cdot|$  denotes the volume of the cube.  $\delta_{\min} = \min\{p_i : p_i = \mathbf{x}(i) - \hat{\mathbf{q}}(i) > 0, 1 \leq i \leq K\}$  and  $\delta_{\max} = \max\{0, p_i : p_i = \hat{\mathbf{q}}(i) - \mathbf{x}(i) \leq 0, 1 \leq i \leq K\}$ , where  $\mathbf{x}(i), \hat{\mathbf{q}}(i)$  denote the  $i$ -th entry of  $\mathbf{x}$  and  $\hat{\mathbf{q}}$ , respectively. Thus, the probability of uniformly drawing a sample  $\mathbf{y}$  belonging to  $A \cap B$  from  $B_\infty(\mathbf{x}, r_{\mathbf{x}})$  is as follows:

$$\begin{aligned}
 Pr(\mathbf{y} \in A \cap B) &\leq \frac{(r_{\mathbf{x}} - \delta_{\min})^{K-C} (r_{\mathbf{x}} + \delta_{\max})^C}{(2r_{\mathbf{x}})^K} \leq \left( \frac{r_{\mathbf{x}} + \delta_{\max}}{r_{\mathbf{x}} - \delta_{\min}} \right)^C 2^{-K} \\
 &= O(2^{-K}).
 \end{aligned} \tag{43}$$

The proof is completed. □

Recall that let  $\mathbb{B} := B(p) \times B_\infty(\mathbf{x}, r_{\mathbf{x}})$  and  $f_{\mathbb{B}}^* := \min_{(p_{\mathbf{y}}, \mathbf{y}) \in \mathbb{B}} f_{p_{\mathbf{y}}}(\mathbf{y})$  for notational simplicity, then

**Proposition B.14 (evaluation efficiency for TnALE).** *Let  $\mathcal{B} \in \mathbb{R}^{I \times I \times \dots \times I}$  be the tensor of order- $(K + 1)$  constructed as Eq. (6) with  $I_1 = I_2 = \dots = I_{K+1} = I$ . Then, there exists its TT-cross approximation (Oseledets & Tyrtshnikov, 2010) of rank- $R^7$ , denoted  $\hat{\mathcal{B}}$ , for which it satisfies  $\mathbf{j} = \arg \max_{\mathbf{i}} \hat{\mathcal{B}}(\mathbf{i})$ , such that the equality  $f_{\mathbb{B}}^* = f_{p_{\mathbf{j}_{K+1}}}(\mathbf{x} + \mathbf{j} : K) - (\lceil r_{\mathbf{x}} \rceil + 1)$  holds, provided that*

$$f_{\mathbb{B}}^* \leq f_{p_{\mathbf{z}}}(\mathbf{z}) / \left( 1 + 2 \frac{(4R)^{\lceil \log_2 K \rceil} - 1}{4R - 1} (R + 1)^2 \xi f_{p_{\mathbf{z}}}(\mathbf{z}) \right) \tag{44}$$

for all  $(p_{\mathbf{z}}, \mathbf{z}) \in \mathbb{B}$  and  $f_{p_{\mathbf{z}}}(\mathbf{z}) \neq f_{\mathbb{B}}^*$ . Here,  $\xi$  denotes the error between  $\mathcal{B}$  and its best approximation of TT-ranks  $R$  in terms of  $\|\cdot\|_\infty$ . Note that the inequality (44) holds trivially if  $\mathcal{B}$  is exactly of the TT topology of rank- $R$ , and Oseledets & Tyrtshnikov (2010) shows that the  $f_{\mathbb{B}}^*$  can be recovered from  $O(KIR)$  entries from  $\mathcal{B}$ .

<sup>7</sup>Here we assume that all elements of the TT-ranks are equal to  $R$  for brevity.

*Proof.* Since the “one-to-one” relation between the entries of the tensor  $\mathcal{B}$  and all possible  $f(\mathbf{z})$  for all  $(p_{\mathbf{z}}, \mathbf{z}) \in B(p) \times B_{\infty}(\mathbf{x}, r_{\mathbf{x}})$ , it is easily to know the equality  $f_{\mathbb{B}}^* = f_{p_{j, K+1}}(\mathbf{x} + \mathbf{j}(: K) - (\lceil r_{\mathbf{x}} \rceil + 1))$  holds if  $\hat{\mathcal{B}}(\mathbf{i}^*) \geq \hat{\mathcal{B}}(\mathbf{k})$  for  $\mathbf{i}^* = \arg \max_{\mathbf{i}} \mathcal{B}(\mathbf{i})$  and any index  $\mathbf{k}$ . To prove this condition true, we have the following inequalities for any  $\mathbf{k}$ :

$$\begin{aligned}
 \hat{\mathcal{B}}(\mathbf{i}^*) - \hat{\mathcal{B}}(\mathbf{k}) &\geq \mathcal{B}(\mathbf{i}^*) - \mathcal{B}(\mathbf{k}) - 2 \frac{(4R)^{\lceil \log_2 K \rceil} - 1}{4R - 1} (R + 1)^2 \xi \\
 &= 1/f_{\mathbb{B}}^* - 1/f_{p_{j, K+1}}(\mathbf{x} + \mathbf{k}(: K) - (\lceil r_{\mathbf{x}} \rceil + 1)) - 2 \frac{(4R)^{\lceil \log_2 K \rceil} - 1}{4R - 1} (R + 1)^2 \xi, \quad (45) \\
 &\geq 2 \frac{(4R)^{\lceil \log_2 K \rceil} - 1}{4R - 1} (R + 1)^2 \xi - 2 \frac{(4R)^{\lceil \log_2 K \rceil} - 1}{4R - 1} (R + 1)^2 \xi = 0
 \end{aligned}$$

where the first inequality follows from Theorem 2 in (Osinsky, 2019), and the last inequality follows from the inequality (44). It can also be known if  $\mathcal{B}$  is exactly of the TT topology of rank- $R$ ,  $\hat{\mathcal{B}}$  is able to recover  $\mathcal{B}$  exactly. In this case  $\xi = 0$  and  $f_{\mathbb{B}}^* \leq f(\mathbf{z})$  trivially for all  $\mathbf{z}$ .  $\square$

## C. Experiment details

### C.1. Low-rank structure of the optimization landscape

To verify the low-rank structure of the optimization landscape of (1), we empirically check the singular values of the landscape tensor using the synthetic data. To be specific, we re-use the fourth-order tensor in the experiment for TN-PS, *i.e.*, TR (order-4) in Table 5. Here we remove the influence of unknown permutations and calculate the objective for all possible combinations of values of the TN-ranks. As a result, for each data, we have a landscape tensor (a tensor whose entries are values of the objective function) of order-4, and the modes of the tensor corresponding to the four TN-ranks. Figure 3 (a) shows the singular values of the landscape tensor unfolded along different modes on average. We see that the landscape tensor provides a *significant* low-rank structure in these data. We also depict the complete landscape (contour line, unfolded along the first two modes) with respect to Data A in Figure 3 (b). We can see that the obviously repeated pattern shown in the figure is the main reason leading to the low-rank structure of the landscape.

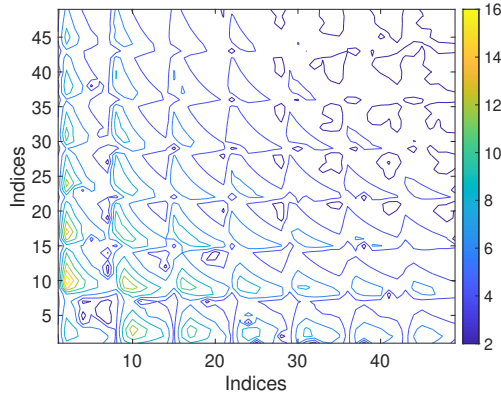
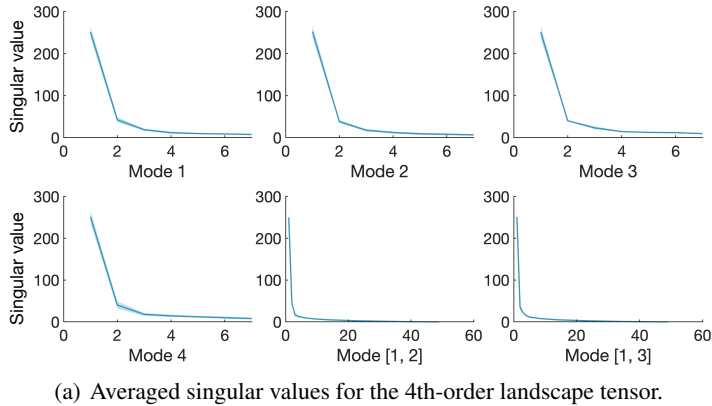


Figure 3. Averaged singular values and Optimization landscapes for the tensor of order-4.

### C.2. Details for the experiment of TN-PS (*w.r.t.*, Table 1).

**Goal.** In this experiment, we intend to verify the superiority of TnALE in solving TN-PS problem.

**Data generation.** For the synthetic data of TR (order-4, order-6, order-8), PEPS (order-6), HT (order-6) and MERA (order-8) topology, we *re-use* the data from (Li et al., 2022). For the generation of data with TW (order-5) structure, we set the dimension of each tensor mode to be 3, meanwhile, the TN-ranks are randomly selected from  $\{1, 2, 3\}$ . Then we *i.i.d.* draw samples from Gaussian distribution  $N(0, 1)$  as the values of core tensors. After contracting these core tensors according to the tensor wheel topology, we uniformly permute the tensor modes at random.

**Settings.** In the experiment, we implement TNGA and TNLS for comparison. For all the methods, we use the same

Table 5. Experimental results of the TN-PS task on TR topology. In the table, *Eff.* and the required evaluation numbers *#Eva.* are demonstrated. Specifically, *#Eva.* is shown in the square brackets.

Methods	Order 4					order 6					order 8				
	A	B	C	D	E	A	B	C	D	E	A	B	C	D	E
	<i>Eff.</i> ↑ [ <i>#Eva.</i> ↓]														
TNGA	1.00 [450]	1.00 [450]	1.17 [450]	1.00 [300]	1.00 [450]	1.00 [1500]	1.00 [1350]	1.00 [1650]	1.16 [1650]	1.00 [1050]	1.00 [2850]	1.02 [2250]	1.11 [3950]	1.06 [1950]	0.88 [1500]
TNLS	1.00 [240]	1.00 [300]	1.17 [60]	1.00 [300]	1.00 [360]	1.00 [660]	1.00 [600]	1.00 [660]	1.16 [600]	1.00 [540]	1.00 [1020]	1.02 [960]	1.11 [1320]	1.06 [780]	1.17 [900]
TnALE(ours)	1.00 [93]	1.00 [155]	1.17 [31]	1.00 [124]	1.00 [62]	1.00 [156]	1.00 [321]	1.00 [156]	1.16 [156]	1.00 [89]	1.00 [231]	1.02 [308]	1.11 [308]	1.06 [231]	1.17 [178]

Table 6. Experimental results of the TN-PS task on PEPS, HT, MERA and TW topology. In the table, *Eff.* and the required evaluation numbers *#Eva.* are demonstrated. Specifically, *#Eva.* is shown in the square brackets. For the approach fail in the experiment, we use “-” to denote it.

Methods	PEPS				HT				MERA				TW			
	A	B	C	D	A	B	C	D	A	B	C	D	A	B	C	D
	<i>Eff.</i> ↑ [ <i>#Eva.</i> ↓]															
TNGA	1.14 [1560]	-	1.00 [840]	1.21 [1080]	1.45 [960]	1.21 [1320]	1.18 [840]	1.29 [1080]	-	1.32 [960]	2.30 [2800]	1.00 [3240]	1.24 [1920]	2.61 [1440]	1.23 [600]	1.30 [720]
TNLS	1.14 [781]	1.00 [781]	1.00 [421]	1.21 [661]	1.45 [841]	1.21 [841]	1.18 [781]	1.29 [721]	1.09 [1561]	1.88 [841]	2.88 [1441]	1.03 [721]	1.24 [661]	2.61 [601]	1.23 [601]	1.30 [481]
TnALE(ours)	1.14 [407]	1.00 [465]	1.00 [233]	1.21 [175]	1.45 [211]	1.21 [281]	1.18 [211]	1.29 [211]	1.09 [1450]	1.88 [484]	2.88 [323]	1.03 [323]	1.24 [285]	2.61 [143]	1.23 [285]	1.30 [214]

objective function as in Li & Sun (2020). Specifically, in the experiment the objective function of (1) is as follows:

$$F(G, \mathbf{r}) = \underbrace{\frac{1}{\epsilon(G, \mathbf{r})}}_{\text{compression ratio (CR)}} + \lambda \cdot \underbrace{\min_{\mathcal{Z} \in TNS(G, \mathbf{r})} \|\mathcal{X} - \mathcal{Z}\|^2 / \|\mathcal{X}\|^2}_{\text{relative square error (RSE)}}, \quad (46)$$

where  $\mathcal{X}$  denotes the synthetic tensor, and  $\epsilon(G, \mathbf{r})$  represents the compression ratio equalling to

$$\epsilon(G, \mathbf{r}) = \frac{\text{Dimension of } \mathcal{X}}{\text{Dimension sum of core tensors of the TN under } (G, \mathbf{r})}.$$

We set the trade-off parameter in (46) to be 200 and for the solver of the inner minimization, we select the Adam optimizer Kingma & Ba (2014) with the learning rate of 0.001 and use Gaussian distribution  $N(0, 0.1)$  to initialize the core tensors. Moreover, the search range for TN-ranks is set from 1 to 7, except for TW data, which is set from 1 to 4. For TNGA, the maximum number of generations is set to be 30. The population in each generation is set to be 120 for all the TN structures except for TR which is set as 150. During each generation in TNGA, the elimination rate is 36% and the reproduction trick (Snyder & Daskin, 2006) is adopted and we set the reproduction number to be 2. Meanwhile, for the selection probability of the recombination operation, we set hyper-parameters  $\alpha = 20$  and  $\beta = 1$ . Moreover, there is a chance of 24% for each gene to mutate after the recombination. For TNLS, we set the sample numbers in each local sampling stage to 60 and the tuning parameter  $c_1 = 0.9$  throughout the experiment. For the tuning parameter  $c_2$ , it is adjusted with tensor order, and we set  $c_2 = 0.9$  for order-4 TR,  $c_2 = 0.94$  for order-6 TR, PEPS, TW and HT, and for MERA and order-8 TR,  $c_2 = 0.98$ . For the proposed method, throughout the experiment, we set the rank-related radius  $r_1 = 2$  and  $r_2 = 1$ . Moreover, we set the number of iterations in the initialization phase to 2 and the number of iterations in the searching phase to 30. For the number of round-trips of ALE, we set it to 1. For performance evaluation, we use the *Eff.* index, and  $Eff. \geq 1$  indicates an identical or more compact structure has been found. For the result fails to satisfy conditions  $RSE \leq 10^{-4}$  and  $Eff. \geq 1$ , we say the approach fails in the experiment.

**Results.** The results of TR topology are demonstrated in Table 5 and the results of PEPS, HT, MERA and TW topology are shown in Table 6. From the results, we can observe that TNLS and TnALE can successfully identify the ranks and permutation of the data with the  $Eff. \geq 1$  which highlight the structure searching ability in the TN-PS task. While compared with TNLS, TnALE achieves the same results with significantly fewer evaluation requirements and it demonstrates the superiority of the TnALE in solving the TN-PS problem. In Figure 4, we illustrate the averaged log objective curves with varying evaluation numbers of TNLS and TnALE. From the figures, we can see that in most cases, TnALE has a faster descending trend and has a lower objective value given the same amount of evaluation numbers. These results imply the advantage of the proposed method in practice, where we have restricted computational resources and can only afford a

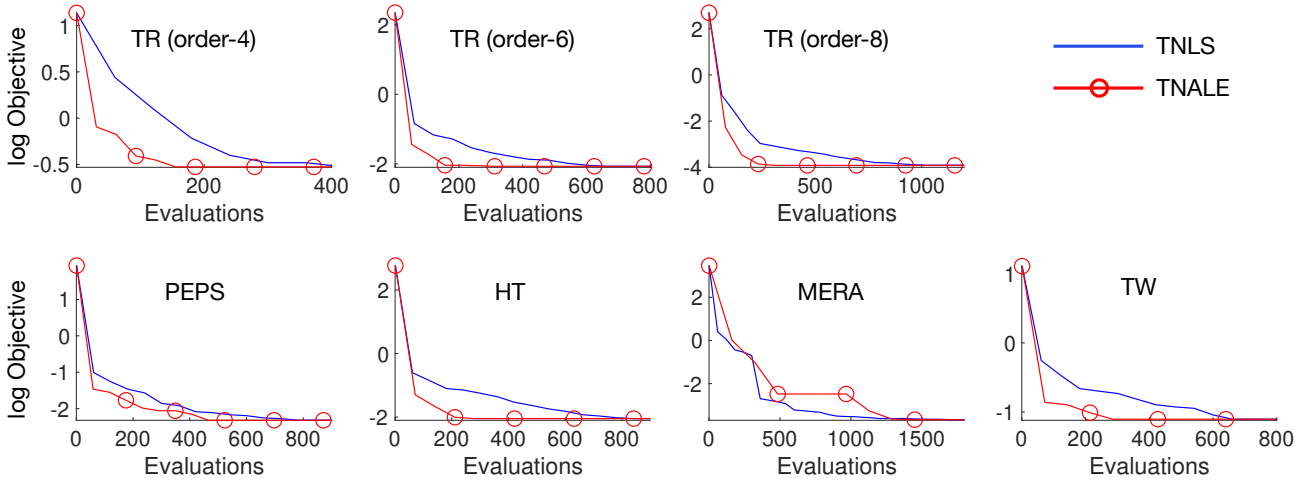


Figure 4. Averaged objective (in the log form) with varying the number of evaluations.

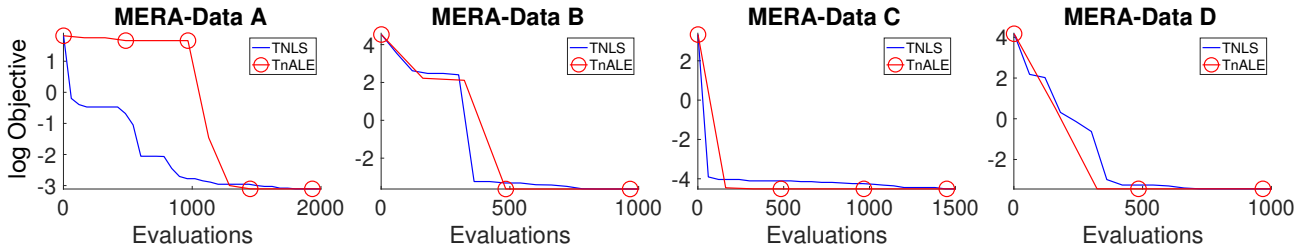


Figure 5. Objective (in the log form) with varying the number of evaluations: an observation of the local convergence of TnALE (Data A).

certain amount of evaluations. For the results of MERA, we further draw the objective curves of each data in Figure 5, from the MERA-Data A curve, we can see that TnALE descends very slowly until around 1000 evaluations while TnALS keeps descending, and the main reason is that TnALE falls into the local optimal and struggles to jump out by restarting the ALE algorithm with a new random center, while TnALS may jump out of it more easily due to its stochastic essence. Moreover, to illustrate how different TN-PS methods scale with tensor order, we draw an average number of evaluations curves with TR order and the results are shown in Figure 6. From the results, we can see that the proposed method increases slower with tensor order compared with other methods, and these results highlight its scalability to tensor order.

### C.3. Details for the experiment of TN-RS (w.r.t. Table 2).

**Goal.** In this experiment, we consider the classic rank-selection problem, *i.e.*, TN-RS, for TR decomposition.

**Data Generation.** We generate the synthetic tensors in TR topology and consider two configurations: “*lower-ranks*” and “*higher-ranks*”. For both configurations, five tensors are generated by randomly choosing ranks and values of vertices (core tensor). The order of each tensor is equal to 8 and the dimensions for each tensor mode are set to equal 3. We *i.i.d.* draw samples from Gaussian distribution  $N(0, 1)$  as the values of vertices. In the “*lower-ranks*” group, we uniformly select the TN-ranks from the interval  $[1, 4]$  in random, while in the “*higher-ranks*” group, the rank interval is lifted to  $[5, 8]$  so that the ranks would be larger than the tensors’ mode dimension. It aims to simulate the scenario of the over-determined ranks, which happens commonly in practice for high-order TNs but is rarely studied in the existing works.

**Settings.** In the experiment, we implement various rank-adaptive TR decomposition methods for comparison, including TR-SVD, TR-rSVD, TR-ALSAR, TR-BALS and TR-BALS2 (Zhao et al., 2016), TR-LM (Alg. 2 and Alg. 3) (Mickelin & Karaman, 2020), TRAR (Sedighin et al., 2021). In addition, the TTOpt algorithm (Sozykin et al., 2022) with ranks<sup>8</sup> equaling 1, 2 is also employed as a baseline. to verify the superiority of the “local-searching” scheme used in TnALE (ours).

<sup>8</sup>Here the ranks are tuning parameters in the TTOpt algorithm.

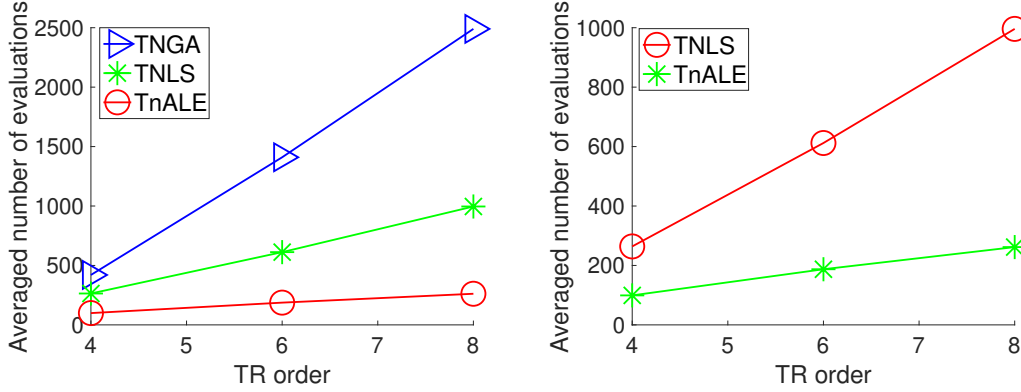


Figure 6. Number of evaluations with varying TR orders.

In more detail, for TR-SVD, TR-rSVD, TR-ALSAR, TR-BALS, and TR-BALS2 (Zhao et al., 2016), the available codes have been used.<sup>9</sup> In these algorithms, in order to obtain a larger  $Eff.$  value, we adjust the parameters  $tol$  and  $MaxIter$  so that the value of  $RSE$  is less than but much closer to  $10^{-4}$ . For TR-LM (Alg. 2 and Alg. 3) (Mickelin & Karaman, 2020), the available codes have been used.<sup>10</sup> and we use the default parameter settings but adjust the value of  $prec$  to obtain a larger  $Eff.$  value. For TRAR (Sedighin et al., 2021), we replace the TR-ALS (Wang et al., 2017) of the *Algorithm 1* in Mickelin & Karaman (2020) with the same decomposition method used in TTOpt. It is because the initialization method of TR-ALS is not suitable for the case of higher ranks. For TTOpt (Sozykin et al., 2022), the objective function is the same as that in the TN-PS experiment and the trade-off parameter  $\lambda = 200$ . For the *lower ranks* group, the rank searching range is set to be  $[1, 7]$ , while for the *higher ranks* group, the range is lifted to  $[1, 10]$ . For the initialization part, we *i.i.d.* draw samples from Gaussian distribution  $N(0, 1)$  as the values of core tensors. For the proposed method, we set rank-related radius  $r_1 = 3, r_2 = 2$  and  $r_1 = 2, r_2 = 1$  for the higher ranks group and lower ranks group respectively. The number of iterations in the initialization phase, the number of iterations in the searching phase and the number of the round-trips of ALE are set to 1, 30 and 1 respectively throughout the experiments. For other parameters of TnALE, we set them the same as TTOpt. For TNGA, we set the population in each generation to be 60, and the searching ranges and core tensors initialization scheme are similar to TTOpt, for the other parameters of TNGA we set them the same as the TN-PS experiment. For TNLS, we set the sample numbers in each local sampling stage to be 60 and  $c_1 = 0.9$ , and the other parameters are set the same as TTOpt. The stop condition is  $RSE \leq 10^{-4}$  and  $Eff. \geq 1$ . In the experiment, we force all approaches to achieve  $RSE \leq 10^{-4}$  and the  $Eff. \geq 1$ , otherwise, we say the approach fails in rank selection.

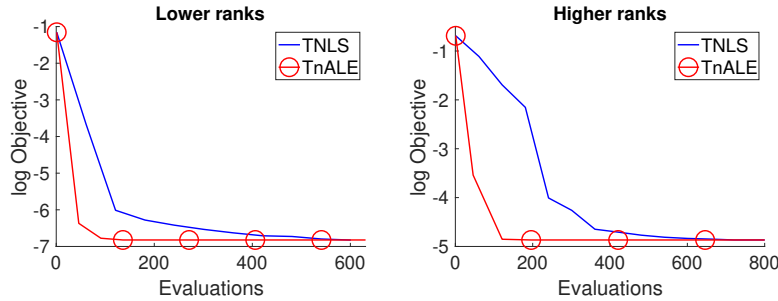


Figure 7. Objective (in the log form) with varying the number of evaluations.

**Results.** As shown in Table 7 and Table 8, in the lower rank regime, TR-BALS, TR-LM (Alg. 2), TTOpt, TNGA, TNLS and TnALE (ours) can successfully select the right TR-ranks (implied by  $Eff. \geq 1$  and  $RSE \leq 10^{-4}$ ), while in the higher rank regime, only TTOpt, TNGA, TNLS and TnALE (ours) manage to find the ranks. Furthermore, TnALE (ours) costs the fewest evaluations compared with TNGA, TNLS and TTOpt which demonstrates the superiority of the TnALE in solving TN-RS problem. To compare the running time of TnALE with TNGA and TNLS, in Figure 8 we demonstrate the average

<sup>9</sup><https://qibinzhao.github.io/>
<sup>10</sup><https://github.com/oscar Mickelin/tensor-ring-decomposition>

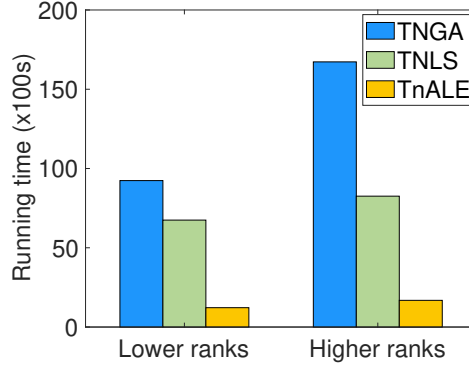


Figure 8. Running time in TN-RS experiment

running time of these methods in lower ranks group and higher ranks group experiments respectively. From the results, we can see that much time has been saved due to the superiority of the TnALE in the number of evaluations. In Figure 7, we illustrate the averaged log objective curves with varying evaluation numbers of TNLS and TnALE. From the figure, we can see that in both configurations, TnALE has a faster descending trend and a lower objective value given the same amount of evaluation numbers. These results imply the advantage of the proposed method in practice, where are restricted computational resources and can only afford a certain amount of evaluations.

C.4. Details for the experiment of knowledge transfer.

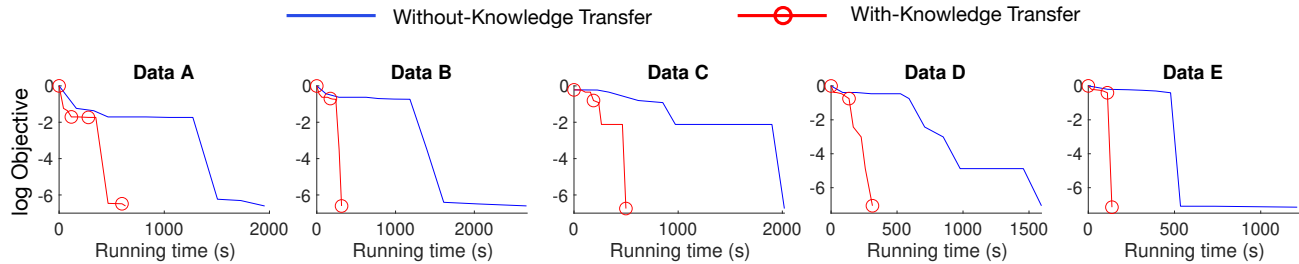


Figure 9. Objective (in the log form) curves with running time

**Goal.** In this experiment, we aim at verifying the acceleration of TnALE when using the knowledge transfer trick.

**Data generation.** In this experiment, we *re-use* the data in the TN-RS experiment, specifically the data from the lower ranks group.

**Settings.** Here, two types of TnALE are implemented, one is TnALE with the knowledge transfer trick and the other is TnALE without the knowledge transfer trick. These two methods use the same parameter settings listed as follows: the rank searching range is set to be  $[1, 7]$ , the trade-off parameter  $\lambda$  is set to 200, rank-related radius  $r_2 = 2$  and we set the number of iterations in the initialization phase to 0 and the number of iterations in the searching phase to 30. For the number of round-trips of ALE, we set it to 1. For the Adam optimizer, the learning rate is set to 0.001 and we use Gaussian distribution  $N(0, 1)$  to initialize the core tensors. Furthermore, these two methods are initialized with the same TN-ranks.

**Results.** The objective curves following the running time are demonstrated in Figure 9. From the figures, we can observe that both methods start with the same log objective but have a big difference in the descending process. Compared with TnALE without the knowledge transfer trick, the objectives of TnALE with the knowledge transfer trick drop rapidly and achieve roughly two times and even almost five times faster than its counterpart.

Table 7. Experimental results of TN-RS (rank selection) in 8-th order TR topology under the "lower ranks" group. In the first column of the table, A, B, C, D, E (*Data*) and their corresponding vectors (*Rank\_grt*) represent the five generated synthetic tensors and the TN-ranks of these five tensors. The item *Rank\_gest* indicates the specific value of the TN-ranks learned by the corresponding method under the constraint  $RSE \leq 10^{-4}$ , and *Time (s)* or *[#Eva.]* indicates the running time or the number of evaluations that the method required.

Methods	TR-SVD			TR-rSVD			TR-ALSAR		
<i>Data</i> [ <i>Rank_grt</i> ]	<i>Eff. / RSE</i>	<i>Rank_est</i>	<i>Time (s)</i>	<i>Eff. / RSE</i>	<i>Rank_est</i>	<i>Time (s)</i>	<i>Eff. / RSE</i>	<i>Rank_est</i>	<i>Time (s)</i>
A [3 4 2 3 1 3 4 2]	0.45 / 8.55E-13	[3 8 4 6 2 6 3 1]	0.0029	0.51 / 0.0013	[3 6 4 6 2 6 3 1]	0.0038	0.08 / 2.43E-05	[11 7 7 7 10 14 8 10]	0.5959
B [3 4 4 2 2 1 1 4]	0.23 / 4.45E-05	[3 9 11 6 6 3 3 1]	0.0081	0.37 / 0.0146	[3 6 6 6 6 3 3 1]	0.0043	0.79 / 4.02E-12	[4 4 4 2 2 2 3 3]	0.0324
C [2 4 2 3 3 1 4 4]	0.29 / 3.55E-05	[3 9 8 4 8 4 3 1]	0.002812	0.46 / 0.0210	[3 6 6 4 6 3 3 1]	0.0039	0.94 / 3.55E-05	[4 4 2 1 2 2 3 4]	0.0333
D [1 4 1 3 4 2 1 1]	<b>1.13 / 4.78E-05</b>	[1 2 1 3 4 2 1]	0.0084	<b>1.13 / 4.78E-05</b>	[1 2 1 3 4 2 1]	0.0055	0.64 / 2.29E-11	[1 3 3 4 4 2 2 1]	0.0233
E [4 1 4 2 3 2 1 1]	<b>1.17 / 2.04E-13</b>	[3 1 3 2 3 2 1 1]	0.0043	<b>1.17 / 3.13E-13</b>	[3 1 3 2 3 2 1 1]	0.0059	0.78 / 1.45E-11	[3 3 3 2 3 2 2 1]	0.0205

Methods	TR-BALS			TR-BALS2			TRAR		
<i>Data</i>	<i>Eff. / RSE</i>	<i>Rank_est</i>	<i>Time (s)</i>	<i>Eff. / RSE</i>	<i>Rank_est</i>	<i>Time (s)</i>	<i>Eff. / RSE</i>	<i>Rank_est</i>	<i>[#Eva.]</i>
A	<b>1.00 / 5.00E-13</b>	[3 4 2 3 1 3 4 2]	0.0146	0.45 / 6.90E-13	[3 8 4 6 2 6 3 1]	0.0188	0.48 / 3.79E-11	[4 4 3 4 5 4 4 3]	69
B	<b>1.07 / 6.07E-13</b>	[3 4 4 2 2 1 1 3]	0.0127	0.20 / 1.03E-05	[3 9 12 6 6 3 3 5]	0.0174	0.61 / 3.17E-08	[3 4 4 4 4 2 4 3]	37
C	<b>1.38 / 3.55E-05</b>	[2 4 2 1 2 1 3 4]	0.0189	0.26 / 3.57E-05	[3 9 8 4 8 4 3 6]	0.0151	0.65 / 3.55E-05	[3 4 3 5 3 3 3 4]	68
D	<b>1.13 / 4.78E-05</b>	[1 2 1 3 4 2 1 1]	0.021	<b>1.13 / 4.78E-05</b>	[1 2 1 3 4 2 1 1]	0.0487	0.41 / 5.55E-05	[4 5 3 3 3 3 2 2]	22
E	<b>1.17 / 6.34E-13</b>	[3 1 3 2 3 2 1 1]	0.0303	<b>1.17 / 9.10E-13</b>	[3 1 3 2 3 2 1 1]	0.0212	0.59 / 2.96E-11	[5 2 3 2 3 2 2 3]	36

Methods	TR-LM (Alg. 3)			TR-LM (Alg. 2)			TTOpt (R = 1)		
<i>Data</i>	<i>Eff. / RSE</i>	<i>Rank_est</i>	<i>Time (s)</i>	<i>Eff. / RSE</i>	<i>Rank_est</i>	<i>Time (s)</i>	<i>Eff. / RSE</i>	<i>Rank_est</i>	<i>[#Eva.]</i>
A	0.40 / 4.22E-13	[6 3 1 3 2 6 8 4]	0.0222	<b>1.00 / 2.86E-14</b>	[3 4 2 3 1 3 4 2]	0.2736	<b>1.00 / 9.41E-07</b>	[3 4 2 3 1 3 4 2]	98
B	0.46 / 2.05E-06	[6 7 3 1 3 2 2 6]	0.0204	<b>1.07 / 1.08E-14</b>	[3 4 4 2 2 1 1 3]	0.2402	<b>1.07 / 2.30E-06</b>	[3 4 4 2 2 1 1 3]	140
C	<b>1.38 / 3.55E-05</b>	[2 4 2 1 2 1 3 4]	0.0227	<b>1.38 / 3.55E-05</b>	[2 4 2 1 2 1 3 4]	0.2503	<b>1.11 / 3.55E-05</b>	[2 4 2 1 2 2 4 4]	56
D	<b>1.13 / 4.78E-05</b>	[1 2 1 3 4 3 1 1]	0.026	<b>1.13 / 4.78E-05</b>	[1 2 1 3 4 2 1 1]	0.2407	<b>1.06 / 4.82E-05</b>	[1 2 1 3 4 2 1 2]	91
E	<b>1.17 / 5.62E-14</b>	[3 1 3 2 3 2 1 1]	0.022	<b>1.17 / 5.62E-14</b>	[3 1 3 2 3 2 1 1]	0.2454	<b>1.17 / 6.61E-11</b>	[3 1 3 2 3 2 1 1]	133

Methods	TTOpt (R = 2)			TTOpt (R = 3)			TNGA		
<i>Data</i>	<i>Eff. / RSE</i>	<i>Rank_est</i>	<i>[#Eva.]</i>	<i>Eff. / RSE</i>	<i>Rank_est</i>	<i>[#Eva.]</i>	<i>Eff. / RSE</i>	<i>Rank_est</i>	<i>[#Eva.]</i>
A	<b>1.00 / 5.00E-06</b>	[3 4 2 3 1 3 4 2]	518	<b>1.00 / 8.93E-05</b>	[3 4 2 3 1 3 4 2]	1533	<b>1.00 / 9.98E-05</b>	[3 4 2 3 1 3 4 2]	480
B	<b>1.02 / 4.86E-07</b>	[3 4 4 2 2 2 1 3]	336	<b>1.02 / 3.72E-06</b>	[3 4 4 2 2 2 1 3]	735	<b>1.07 / 9.95E-05</b>	[3 4 4 2 2 1 1 3]	660
C	<b>1.02 / 3.56E-05</b>	[2 5 2 2 3 1 3 5]	154	<b>1.00 / 9.45E-05</b>	[2 5 2 2 3 2 3 4]	273	<b>1.11 / 9.95E-05</b>	[2 4 2 1 2 2 4 4]	600
D	<b>1.06 / 1.10E-08</b>	[1 3 1 3 4 2 1 1]	196	<b>1.00 / 4.87E-05</b>	[1 2 1 3 4 2 1 3]	483	<b>1.06 / 9.98E-05</b>	[1 2 1 3 4 2 1 2]	600
E	<b>1.03 / 7.94E-06</b>	[3 1 3 2 3 3 1 1]	364	<b>1.17 / 3.14E-11</b>	[3 1 3 2 3 2 1 1]	1071	<b>1.17 / 9.92E-05</b>	[3 1 3 2 3 2 1 1]	420

Methods	TNLS			TnALE (ours)		
<i>Data</i>	<i>Eff. / RSE</i>	<i>Rank_est</i>	<i>[#Eva.]</i>	<i>Eff. / RSE</i>	<i>Rank_est</i>	<i>[#Eva.]</i>
A	<b>1.00 / 9.99E-05</b>	[3 4 2 3 1 3 4 2]	600	<b>1.00 / 9.98E-05</b>	[3 4 2 3 1 3 4 2]	66
B	<b>1.07 / 9.97E-05</b>	[3 4 4 2 2 1 1 3]	420	<b>1.07 / 9.98E-05</b>	[3 4 4 2 2 1 1 3]	99
C	<b>1.11 / 9.99E-05</b>	[2 4 2 1 2 2 4 4]	420	<b>1.11 / 9.95E-05</b>	[2 4 2 1 2 2 4 4]	99
D	<b>1.06 / 9.97E-05</b>	[1 2 1 3 4 2 1 2]	480	<b>1.06 / 9.98E-05</b>	[1 2 1 3 4 2 1 2]	69
E	<b>1.17 / 9.92E-05</b>	[3 1 3 2 3 2 1 1]	540	<b>1.17 / 9.93E-05</b>	[3 1 3 2 3 2 1 1]	63

### C.5. Details for the experiment of TGP (*w.r.t.* Table 3).

**Goal.** In this experiment, we aim to use the proposed method to compress the learnable parameters of the TGP (Izmailov et al., 2018).

**Data generation.** In this task, we choose three univariate regression datasets from the UCI and LIBSVM archives. The Combined Cycle Power Plant (CCPP)<sup>11</sup> dataset consists of 9569 data points collected from a power plant with 4 features and a single response. The MG<sup>12</sup> data have 1385 data points with 6 features and a single response. The Protein<sup>13</sup> data contain 45730 instances with 9 attributes and a single response. For all the datasets, we randomly choose 80% of the data for training and the rest for testing, then standardize the training and testing sets respectively by removing the mean and scaling to unit variance. For CCPP, we choose 12 inducing points on each feature and result in an order-4 tensor of shape  $12 \times 12 \times 12 \times 12$ . For MG, we choose 8 inducing points and get an order-6 tensor of shape  $8 \times 8 \times 8 \times 8 \times 8 \times 8$ . For Protein, we choose 4 inducing points and obtain an order-9 tensor of shape  $4 \times 4 \times 4$ . For all the datasets, the TT-ranks for the TGP (Izmailov et al., 2018) algorithm is set to 10. To learn more compact representations, we apply the TN-PS algorithms to TGP. In particular, we first train a TGP with given TT-ranks and get the TT representation of the variational mean. Then we use the TN-PS algorithms to search for alternative structures of the TT variational mean and compress the parameter numbers.

**Settings.** For all the comparing methods, we use the same objective function as in the TN-PS experiment and we set  $\lambda = 1 \times 10^5, 1 \times 10^7, 1 \times 10^3$  for CCPP, MG and Protein, respectively. Moreover, the rank searching range, the learning rate of Adam, and the variance of the Gaussian distribution for core tensors initialization are set from 1 to 14, 0.001, and

<sup>11</sup><https://archive.ics.uci.edu/ml/datasets/Combined+Cycle+Power+Plant>

<sup>12</sup><https://www.csie.ntu.edu.tw/~cjlin/libsvmtools/datasets/regression.html#mg>

<sup>13</sup><https://archive.ics.uci.edu/ml/datasets/Physicochemical+Properties+of+Protein+Tertiary+Structure>

Table 8. Experimental results of TN-RS (rank selection) in 8-th order TR topology under the "higher ranks" group. In the first column of the table, A, B, C, D, E (*Data*) and their corresponding vectors (*Rank\_grt*) represent the five generated synthetic tensors and the TN-ranks of these five tensors. The item *Rank\_gest* indicates the specific value of the TN-ranks learned by the corresponding method under the constraint  $RSE \leq 10^{-4}$ , and *Time (s)* or *[#Eva.]* indicates the running time or the number of evaluations that the method required.

Methods	TR-SVD				TR-rSVD				TR-ALSAR			
<i>Data</i> [ <i>Rank_grt</i> ]	<i>Eff. / RSE</i>	<i>Rank_est</i>	<i>Time (s)</i>	<i>Eff. / RSE</i>	<i>Rank_est</i>	<i>Time (s)</i>	<i>Eff. / RSE</i>	<i>Rank_est</i>	<i>Time (s)</i>	<i>Eff. / RSE</i>	<i>Rank_est</i>	<i>Time (s)</i>
A [8 8 8 5 7 6 8 8]	0.16 / 9.40E-05	[3 9 27 38 27 9 3 1]	0.0174	0.16 / 9.40E-05	[3 9 27 38 27 9 3 1]	0.0238	1.11 / 0.0172	[7 7 7 6 6 6 8 8]	11.2686			
B [6 5 7 7 6 5 6 5]	0.12 / 4.30E-05	[3 9 27 35 26 9 3 1]	0.0136	0.11 / 1.13E-28	[3 9 27 35 27 9 3 1]	0.0361	0.82 / 0.0133	[7 5 6 8 6 6 8 6]	10.536			
C [8 7 7 8 7 5 8 7]	0.12 / 8.32E-05	[3 9 27 51 27 9 3 1]	0.0378	0.12 / 8.32E-05	[3 9 27 51 27 9 3 1]	0.0308	0.71 / 0.0094	[9 8 6 17 6 7 9 8]	16.2148			
D [6 6 6 8 6 7 6 5]	0.13 / 9.64E-05	[3 9 26 38 26 9 3 1]	0.0092	0.12 / 5.32E-05	[3 9 27 38 27 9 3 1]	0.0308	0.63 / 9.62E-05	[9 8 8 8 7 9 7 7]	0.6589			
E [6 6 6 6 5 6 6 6]	0.11 / 4.51E-05	[3 9 27 36 26 9 3 1]	0.0061	0.11 / 5.63E-05	[3 9 27 35 27 9 3 1]	0.0242	0.75 / 0.0298	[7 7 5 6 4 9 8 8]	11.5233			

Methods	TR-BALS				TR-BALS2				TRAR			
<i>Data</i>	<i>Eff. / RSE</i>	<i>Rank_est</i>	<i>Time (s)</i>	<i>Eff./RSE</i>	<i>Rank_est</i>	<i>Time (s)</i>	<i>Eff. / RSE</i>	<i>Rank_est</i>	<i>[#Eva.]</i>			
A	0.03 / 6.04E-29	[28 20 19 26 44 89 51 39]	0.8749	0.16 / 8.39E-05	[3 9 27 39 27 9 3 1]	0.142	0.67 / 5.59E-14	[10 8 8 8 8 10 8 11]	76			
B	0.57 / 9.25E-05	[6 6 10 9 9 7 9 6]	0.0941	0.12 / 9.89E-05	[3 9 27 35 26 9 3 1]	0.1608	0.71 / 1.82E-13	[8 5 7 7 7 6 9 9]	74			
C	0.12 / 9.71E-05	[15 20 18 15 17 19 23 25]	0.2763	0.12 / 6.35E-05	[3 9 27 54 27 9 3 1]	0.1643	0.58 / 8.89E-14	[12 7 10 8 9 10 9 10]	143			
D	0.19 / 8.18E-05	[9 15 17 22 10 16 15 10]	0.1773	0.12 / 9.75E-06	[3 9 27 40 26 9 3 1]	0.1704	0.57 / 3.75E-14	[11 6 7 8 8 9 7 10]	76			
E	0.03 / 3.97E-05	[38 55 59 20 18 15 19 27]	0.446	0.11 / 6.40E-30	[3 9 27 36 27 9 3 1]	0.1749	0.62 / 2.05E-14	[10 6 7 7 7 8 6 9]	75			

Methods	TR-LM (Alg. 3)				TR-LM (Alg. 2)				TTOpt (R = 1)			
<i>Data</i>	<i>Eff. / RSE</i>	<i>Rank_est</i>	<i>Time (s)</i>	<i>Eff. / RSE</i>	<i>Rank_est</i>	<i>Time (s)</i>	<i>Eff. / RSE</i>	<i>Rank_est</i>	<i>[#Eva.]</i>			
A	0.16 / 9.40E-05	[3 9 27 38 27 9 3 1]	0.0257	0.16 / 2.87E-05	[3 9 27 39 27 9 3 1]	0.3318	<b>1.00 / 3.65E-07</b>	[8 8 8 5 7 6 8 8]	220			
B	0.12 / 4.30E-05	[3 9 27 35 26 9 3 1]	0.001	0.15 / 8.36E-05	[3 1 3 9 26 25 25 9]	0.3336	<b>1.00 / 1.52E-07</b>	[6 5 7 7 6 5 6 5]	220			
C	0.12 / 8.32E-05	[3 9 27 51 27 9 3 1]	0.0303	0.17 / 7.07E-05	[3 1 3 9 27 34 27 9]	0.3285	<b>1.00 / 1.01E-06</b>	[8 7 7 8 7 5 8 7]	150			
D	0.13 / 9.64E-05	[3 9 26 38 26 9 3 1]	0.023	0.13 / 9.31E-05	[35 27 9 3 1 3 9 25]	0.3173	<b>1.00 / 1.83E-06</b>	[6 6 6 8 6 7 6 5]	150			
E	0.11 / 4.51E-05	[3 9 27 36 26 9 3 1]	0.0299	0.13 / 9.38E-05	[20 26 9 3 1 3 9 26]	0.3845	<b>1.00 / 5.01E-07</b>	[6 6 6 6 5 6 6 6]	150			

Methods	TTOpt (R = 2)				TTOpt (R = 3)				TNGA			
<i>Data</i>	<i>Eff. / RSE</i>	<i>Rank_est</i>	<i>[#Eva.]</i>	<i>Eff. / RSE</i>	<i>Rank_est</i>	<i>[#Eva.]</i>	<i>Eff. / RSE</i>	<i>Rank_est</i>	<i>[#Eva.]</i>			
A	<b>1.00 / 6.49E-07</b>	[8 8 8 5 7 6 8 8]	540	<b>1.00 / 5.88E-07</b>	[8 8 8 5 7 6 8 8]	1710	<b>1.00 / 9.99E-05</b>	[8 8 8 5 7 6 8 8]	1020			
B	<b>1.00 / 1.61E-07</b>	[6 5 7 7 6 5 6 5]	1060	<b>1.00 / 4.00E-07</b>	[6 5 7 7 6 5 6 5]	2670	<b>1.00 / 9.94E-05</b>	[6 5 7 7 6 5 6 5]	660			
C	<b>1.00 / 1.32E-06</b>	[8 7 7 8 7 5 8 7]	780	<b>1.00 / 9.23E-07</b>	[8 7 7 8 7 5 8 7]	1740	<b>1.00 / 9.95E-05</b>	[8 7 7 8 7 5 8 7]	1380			
D	<b>1.00 / 3.40E-07</b>	[6 6 6 8 6 7 6 5]	540	<b>1.00 / 1.67E-06</b>	[6 6 6 8 6 7 6 5]	1710	<b>1.00 / 9.93E-05</b>	[6 6 6 8 6 7 6 5]	1020			
E	<b>1.00 / 8.02E-13</b>	[6 6 6 6 5 6 6 6]	840	<b>1.00 / 1.99E-07</b>	[6 6 6 6 5 6 6 6]	1740	<b>1.00 / 9.94E-05</b>	[6 6 6 6 5 6 6 6]	420			

Methods	TNLS				TnALE (ours)			
<i>Data</i>	<i>Eff. / RSE</i>	<i>Rank_est</i>	<i>[#Eva.]</i>	<i>Eff. / RSE</i>	<i>Rank_est</i>	<i>[#Eva.]</i>	<i>Eff. / RSE</i>	<i>Rank_est</i>
A	<b>1.00 / 9.97E-05</b>	[8 8 8 5 7 6 8 8]	540	<b>1.00 / 9.96E-05</b>	[8 8 8 5 7 6 8 8]	115		
B	<b>1.00 / 9.92E-05</b>	[6 5 7 7 6 5 6 5]	720	<b>1.00 / 9.91E-05</b>	[6 5 7 7 6 5 6 5]	85		
C	<b>1.00 / 9.91E-05</b>	[8 7 7 8 7 5 8 7]	480	<b>1.00 / 1.00E-04</b>	[8 7 7 8 7 5 8 7]	150		
D	<b>1.00 / 9.93E-05</b>	[6 6 6 8 6 7 6 5]	600	<b>1.00 / 9.92E-05</b>	[6 6 6 8 6 7 6 5]	160		
E	<b>1.00 / 9.92E-05</b>	[6 6 6 6 5 6 6 6]	600	<b>1.00 / 9.93E-05</b>	[6 6 6 6 5 6 6 6]	85		

0.01, respectively. Then for TNGA, the maximum number of generations is set to be 30. The population in each generation is set to be 150, 190, and 300 for the TT variational mean of CCPP, MG, and Protein regression task. The elimination rate is 30% and the reproduction number is set to 1. Moreover, we set  $\alpha = 20$  and  $\beta = 1$ . The chance for each gene to mutate after the recombination is 30%. For TNLS, we set the maximum iteration to 20, and tuning parameters  $c_1 = 0.9$ ,  $c_2 = 0.9$ , and the number of samples in the local sampling stage to 150, 300, 300 for the TT variational mean of CCPP, MG and Protein regression task. For the proposed method, throughout the experiment, we set the rank-related radius  $r_1 = 3$  and  $r_2 = 2$ . Moreover, we set the number of iterations in the initialization phase to 2 and the number of iterations in the searching phase to 30. For the number of round-trips of ALE, we set it to 1. After the TN-PS algorithms, we plug the reparameterized variational mean back into the original TGP model for inference and we evaluate the results by mean squared error (MSE) of the regression tasks on the test datasets.

### C.6. Details for the experiment of natural images compression (w.r.t. Table 4).

**Goal.** In this experiment, we consider using the proposed framework to solve TN-PS and TN-TS tasks for natural image compression.

**Data generation.** In the experiment, we randomly select 4 natural images from the BSD500 (Arbelaez et al., 2010)<sup>14</sup>. The images used in this experiment are demonstrated in Figure 10. We use the Matlab commands "resize" and "rgb2gray" to turn these into grayscale images of size  $256 \times 256$ , and then rescale them to  $[0, 1]$ . Then we use the Matlab command "reshape" to directly reshape these images into order-8 tensors of size  $4 \times 4 \times 4 \times 4 \times 4 \times 4 \times 4 \times 4$ .

**Settings.** In the TN-PS part, we use the same objective function as in the TN-PS experiment and we set  $\lambda = 5$ . Moreover, the rank searching range, the learning rate of Adam, and the variance of the Gaussian distribution for core tensors initialization

<sup>14</sup><https://www2.eecs.berkeley.edu/Research/Projects/CS/vision/bsds/BSDS300/html/dataset/images.html>



Figure 10. Illustration of the employed images in natural images compression experiment.

are set from 1 to 14, 0.01, and 0.1, respectively. For TNLS, we set the maximum number of iterations to 20, and tuning parameters  $c_1 = 0.95$ ,  $c_2 = 0.9$ , and the number of samples in the local sampling stage to 150. For TNGA, the maximum number of generations is set to be 30. The population in each generation is set to be 300. The elimination rate is 10% and the reproduction number is set to 1. Moreover,  $\alpha = 25$ ,  $\beta = 1$ , and we set a 30% chance for each gene to mutate after the recombination is finished. For the proposed method, we set the rank-related radius  $r_1 = 3$  and  $r_2 = 2$ . Moreover, we set the number of iterations in the initialization phase to 1 and the number of iterations in the searching phase to 30. For the number of round-trips of ALE, we set it to 1. In the TN-TS part, the setting of the objective function, the learning rate of Adam, and the variance of the Gaussian distribution for core tensors initialization are set as the same as the TN-PS part and for the rank searching range, we set from 1 to 4. For TNLS, we set the maximum number of iterations to 20, tuning parameters  $c_1 = 0.99$ , and the number of samples in the local sampling stage to 100. For the parameter settings of TNGA, we only change the population number to 100 compared with the TN-PS part. For the proposed method, the rank-related radius  $r_2$  is set to be 1 and we set the number of iterations in the initialization phase to 0 and the number of iterations in the searching phase to 30. For the number of round-trips of ALE, we set it to 1. For Greedy, we set the RSE threshold for stopping the algorithm the same as the result RSE of the proposed method.